

Evolution of pure hydrocarbon hosts: simpler structure, higher performance and universal application in RGB phosphorescent organic light-emitting diodes

Qiang Wang,^{‡a} Fabien Lucas,^b Cassandre Quinton,^b Yang-Kun Qu,^a Joëlle Rault-Berthelot,^b Olivier Jeannin,^b Sheng-Yi Yang,^a Fan-Cheng Kong,^a Sarvendra Kumar,^a Liang-Sheng Liao,^a Cyril Poriel^{*b} and Zuo-Quan Jiang,^{*a}

^a*Institute of Functional Nano & Soft Materials (FUNSOM), Jiangsu Key Laboratory for Carbon-Based Functional Materials & Devices, Soochow University, Suzhou, Jiangsu 215123, China. E-mail: zqjiang@suda.edu.cn.*

^b*Address here. Univ Rennes, CNRS, ISCR- UMR 6226, F-35000 Rennes, France. E-mail: Cyril.poriel@univ-rennes1.fr.*

[‡] Present address: Institut für Physik and IRIS Adlershof, Humboldt-Universität zu Berlin, Brook-Taylor-Str. 6, 12489 Berlin, Germany

Keywords: universal host materials, RGB phosphorescent organic light-emitting diode, spirobifluorene, pure aromatic hydrocarbon, triplet energy

TABLE OF CONTENTS

1	General experimental methods	3
1.1	Synthesis	3
1.2	Spectroscopic studies	3
1.3	Electrochemical studies	4
1.4	Molecular modelling	4
1.5	Thermal analysis	4
1.6	Device fabrication and characterization	5
2	Syntheses of materials	5
2.1	3-Phenyl-9,9'-spirobifluorene [mSPh]	7
2.2	3-Terphenyl-9,9'-spirobifluorene [mSTPh]	7
2.3	3,6-Diphenyl-9,9'-spirobifluorene [mSPh₂]	7
2.4	3,6-diterphenyl-9,9'-spirobifluorene [mSTPh₂]	8
3	Structural properties	9
4	Thermal properties	10
5	Photophysical properties	10
6	Electrochemical studies	11
7	Molecular modelling	13
8	Charge Transport	28
9	Phosphorescent OLED characteristics	28
10	Copy of NMR spectra	31
10.1	mSTPh – ¹ H – CD ₂ Cl ₂	31
10.2	mSTPh – ¹³ C – CD ₂ Cl ₂	32
10.3	mSTPh – ¹³ C – DEPT135 – CD ₂ Cl ₂	33
10.4	mSPh₂ – ¹ H – CD ₂ Cl ₂	40
10.5	mSPh₂ – ¹³ C – CD ₂ Cl ₂	41
10.6	mSPh₂ – ¹³ C – DEPT135 – CD ₂ Cl ₂	42
10.7	mSTPh₂ – ¹ H – CD ₂ Cl ₂	43
10.8	mSTPh₂ – ¹³ C – CD ₂ Cl ₂	44
10.9	mSTPh₂ – ¹³ C – DEPT135 – CD ₂ Cl ₂	45
11	References	52

1 General experimental methods

1.1 Synthesis

All manipulations of oxygen and moisture-sensitive materials were conducted with a standard Schlenk technique. Commercially available reagents and solvents were used without further purification other than those detailed below. THF was obtained through a PURE SOLV™ solvent purification system. Light petroleum refers to the fraction with bp 40-60°C. Analytical thin layer chromatography was carried out using aluminum backed plates coated with Merck Kieselgel 60 GF254 and visualized under UV light (at 254 and 360 nm). Flash chromatography was carried out using Teledyne Isco CombiFlash® Rf 400 (UV detection 200-360 nm), over standard silica cartridges (Redisep® Isco or Puriflash® columns Interchim). ¹H and ¹³C NMR spectra were recorded using Bruker 300 MHz or 400 MHz instruments (¹H frequency, corresponding ¹³C frequency: 75 MHz or 101 MHz); chemical shifts were recorded in ppm and J values in Hz. The residual signals for the NMR solvents used are 5.32 or 7.26 ppm (proton); 53.84 or 77.09 ppm (carbon) for CD₂Cl₂ or CDCl₃, respectively.¹ Mass spectroscopy was performed using a Thermo Fisher ISQ Single Quadrupole GC-MS with direct probe system. High resolution mass spectra were recorded at the Centre Régional de Mesures Physiques de l'Ouest (CRMPO-Rennes) on a Bruker MaXis 4G.

1.2 Spectroscopic studies

UV-visible spectra were recorded using an UV-vis spectrophotometer (Lambda 750) in toluene. Molar absorption coefficients (ϵ) were calculated from the gradients extracted from the plots of absorbance vs concentration with five solutions of different concentrations for each sample.

The fluorescent and phosphorescent (liquid nitrogen) spectra were tested by Hitachi F-4600 spectrophotometer, both in in toluene solution. The excitation wavelength was 290 nm for both, modulated by a monochromator. Triplet energy levels were calculated from the maximum of the first phosphorescence emission peak, and conversion in electron-volt was

obtained with the following formula: $E_T(\text{eV}) = \frac{hc}{\lambda}$ with $h = 6.62607 \times 10^{-34}$ J.s, $c = 2.99792 \times 10^{17}$ nm s⁻¹ and $1 \text{ J} = 1.60218 \times 10^{-19}$ eV. This equation can be simplified as: $E_T(\text{eV}) = \frac{1239.84}{\lambda}$ with λ formulated in nm.

The transient decay PL characteristics were evaluated using a HAMAMATSU (C11637) compact fluorescence lifetime spectrometer under a excitation light wavelength of 373 nm.

1.3 Electrochemical studies

Electrochemical experiments were performed under argon atmosphere using a Pt disk electrode (diameter 1 mm). The counter electrode was a vitreous carbon rod. The reference electrode was either a silver wire in a 0.1 M AgNO₃ solution in CH₃CN for the studies in oxidation or a Silver wire coated by a thin film of AgI (silver(I)iodide) in a 0.1 M Bu₄NI solution in DMF for the studies in reduction. Ferrocene was added to the electrolyte solutions at the end of a series of experiments. The ferrocene/ferrocenium (Fc/Fc⁺) couple served as internal standard. The three electrodes cell was connected to a PAR Model 273 potentiostat/galvanostat (PAR, EG&G, USA) monitored with the ECHEM Software. Activated Al₂O₃ was added in the electrolytic solution to remove excess moisture. All potentials are referred to the SCE electrode that was calibrated at -0.405 V vs. Fc/Fc⁺ system. We estimated the electron affinity (EA) or lowest unoccupied molecular orbital (LUMO) and the ionization potential (IP) or highest occupied molecular orbital (HOMO) from the redox data.²⁻⁴ The LUMO level was calculated from: LUMO (eV) = - [E_{onset}^{red} (vs SCE) + 4.4] and the HOMO level from: HOMO (eV) = - [E_{onset}^{ox} (vs SCE) + 4.4], based on an SCE energy level of 4.4 eV relative to the vacuum. The electrochemical gap was calculated from: ΔE^{el} = |HOMO - LUMO| (in eV).

1.4 Molecular modeling

Full geometry optimization of the ground state (S₀) and frequency calculation were performed with Density Functional Theory (DFT)^{5, 6} using the hybrid Becke-3 0 parameter exchange functional^{7, 8} and the Lee-Yang-Parr non-local correlation functional⁹ (B3LYP) implemented in the Gaussian 16 (Revision B.01) program suite using the 6-31G(d) basis set and the default convergence criterion implemented in the program.

Geometry optimization of the first excited triplet state (E_{T1}) was performed using Time-Dependent Density Functional Theory (TD-DFT) calculations using the B3LYP functional and the 6-31+G(d) basis set.

Infrared spectra were calculated on the final geometry to verify that an energy minimum was reached (i.e. no negative frequency).

Transition diagrams were obtained through TD-DFT calculations performed using the B3LYP functional and the extended 6-311+G(d,p) basis set on the geometry of S₀.

T₁ to S₀ energy transition (ET) was calculated from the difference between the total energy of the molecule in its respective excited triplet state (found through TD-DFT, B3LYP 6-

311+G(d,p)) and its ground singlet state (found through DFT, B3LYP 6-311+G(d,p)) in their optimized geometries.

Spin density (SD) representation was obtained through TD-DFT calculations performed using the extended 6-311+G(d,p) basis set and a triplet spin on the previously optimized geometry of T₁.

Calculations were carried out on the *OCCIGEN* calculator of the *Centre Informatique National de l'Enseignement Supérieur* (CINES (Montpellier) under project No. 2018-A0040805032). Figures were generated with GaussView 6.0 and GaussSum 3.0.

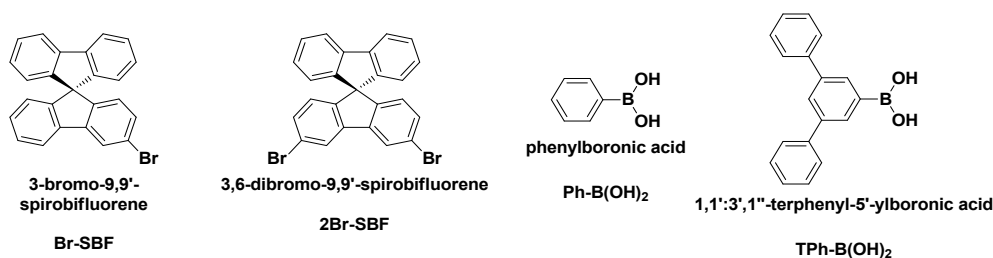
1.5 Thermal analysis

Thermal Gravimetric Analysis (TGA) was carried out by using a TA SDT 2960 instrument. TGA curves were measured at 10 °C min⁻¹ from 30 °C to 800 °C under a nitrogen flux. Differential Scanning Calorimetry (DSC) was carried out by using a TA DSC 2010 unit instrument equipped with an intracooler. DSC traces were measured at 10 °C min⁻¹, 2 heating/cooling cycles were successively carried out under a nitrogen flux.

1.6 Device fabrication and characterization

All organic compounds except the product of this paper were purchased from Lumtec Co., Ltd. ITO substrates (185 nm, R_□ = 10 Ω □⁻¹ for blue PhOLEDs, 135 nm, R_□ = 15 Ω □⁻¹ for green PhOLEDs, 110 nm, R_□ = 18 Ω □⁻¹ for red PhOLEDs; activating area 0.1 cm²; glass substrate, 32 mm × 32 mm × 0.7 mm) with patterned electrodes were ultrasonically cleaned in deionized water, acetone and ethanol for 15 min. Before loading to the vacuum chamber, the substrates were treated by UV ozone for 15 min at 40 °C. OLED devices were fabricated by depositing materials in a thermal evaporator chamber under a vacuum of 4.0 × 10⁻⁶ Torr. The organic layers and cathode were defined by shallow masks placed under the substrates (0.15 cm²), which define an active area of 0.1 cm². The evaporation rates and thicknesses of organic layers (2–4 Å s⁻¹) and aluminum cathode (4–8 Å s⁻¹) was monitored with oscillating quartz crystals. The devices were well encapsulated with glued glass lids before testing. A programmable spectra scan photometer (PHOTO RESEARCH, PR 655) connected to a KEITHLEY 2400 source meter was used to test the EL and luminescence characteristics, and the current–voltage characteristics.

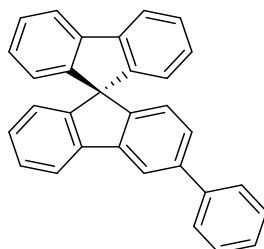
2 Syntheses of materials



The above chemical intermediates were purchased from Suzhou Ge'Ao New Materials Co., Ltd and used without further purification. The four materials are synthesized in same condition by combining bromo spiro compound and boronic acid in a one-step typical method:

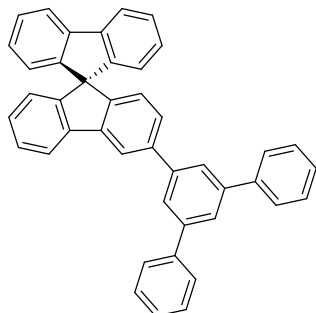
To a round bottom flask was charged Br-SBF (1 mmol, 1 eq), Ph-B(OH)₂ (1.1 mmol, 1.1 eq), K₂CO₃ (3 mmol, 3 eq), Pd(PPh₃)₄ (0.04 mmol, 4% eq) and THF/H₂O (4 ml/1.5 ml). The reaction mixture was refluxed under argon for 12 h. After cooling to r.t., it was diluted with brine (6 mL) and extracted with CH₂Cl₂ (3 × 10 mL). The organic layer was then dried with Na₂SO₄ and the solvent was removed under reduced pressure. All the products were purified by silica gel column chromatography (20% CH₂Cl₂ in petroleum ether).

2.1 3-Phenyl-9,9'-spirobifluorene [*m*SPh]



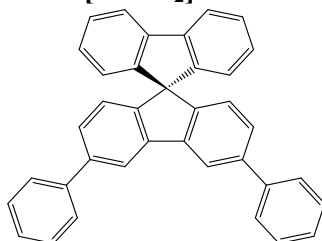
4.5 g of white solid was obtained, yield 92%; ¹H NMR (300 MHz, CD₂Cl₂) δ = 8.11 (dd, *J* = 1.8, 0.6 Hz, 1H), 7.96 (dt, *J* = 7.7, 1.0 Hz, 1H), 7.91 (dt, *J* = 7.6, 0.9 Hz, 2H), 7.75–7.63 (m, 2H), 7.55–7.30 (m, 7H), 7.15 (tdd, *J* = 7.5, 2.5, 1.1 Hz, 3H), 6.80–6.69 (m, 4H); ¹³C NMR (75 MHz, CD₂Cl₂) δ = 149.73 (C), 149.28 (2C), 148.51 (C), 143.07 (C), 142.42 (2C), 142.24 (C), 141.79 (C), 141.69 (C), 129.39 (2CH), 128.58 (CH), 128.44 (2CH), 128.42 (3CH), 127.95 (CH), 127.76 (2CH), 127.54 (CH), 124.58 (CH), 124.41 (CH), 124.40 (2CH), 120.79 (CH), 120.75 (2CH), 119.38 (CH), 66.35 (Cspiro); HRMS calculated for C₃₁H₂₁: 393.16433, found: 393.16378 [M+H]⁺; elemental analysis calculated for C₃₁H₂₀: C, 94.86; H, 5.14; found: C, 94.39; H, 5.03.

2.2 3-Terphenyl-9,9'-spirobifluorene [*m*STPh]



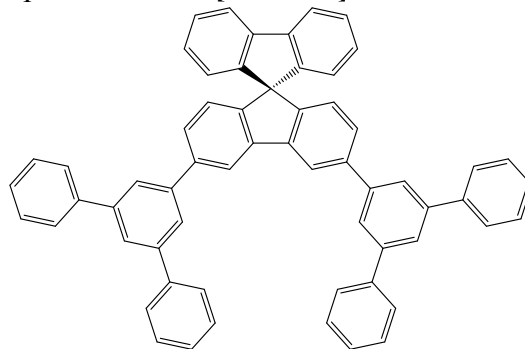
7.1 g of white solid was obtained, yield 96%; ^1H NMR (400 MHz, CDCl_3) δ 8.18 (d, $J = 1.7$ Hz, 1H), 7.96 (d, $J = 7.6$ Hz, 1H), 7.92–7.88 (m, 4H), 7.85 (t, $J = 1.7$ Hz, 1H), 7.79–7.74 (m, 4H), 7.53 (dd, $J = 8.4, 6.8$ Hz, 4H), 7.48–7.39 (m, 6H), 7.17 (td, $J = 7.5, 1.1$ Hz, 3H), 6.87 (d, $J = 7.9$ Hz, 1H), 6.84 (d, $J = 7.6$ Hz, 2H), 6.80 (d, $J = 7.6$ Hz, 1H). ^{13}C NMR (101 MHz, CDCl_3) δ 149.22 (Cqar), 148.73 (2Cqar), 148.28 (Cqar), 142.60 (Cqar), 142.42 (2Cqar), 141.85 (2Cqar), 141.59 (Cqar), 141.21 (2Cqar), 141.09 (Cqar), 128.94 (4CH), 128.14 (CH), 127.96 (2CH), 127.86 (2CH), 127.64 (2CH), 127.44 (4CH), 127.31 (CH), 125.39 (2CH), 125.26 (CH), 124.39 (CH), 124.16 (2CH), 120.11 (2CH), 119.02 (CH), 65.84 (Cspiro); MS (EI) calculated for $\text{C}_{34}\text{H}_{21}\text{N}_3\text{O}$: 544.70, found: 544.09 $[\text{M}]^+$; elemental analysis calculated for $\text{C}_{43}\text{H}_{28}$: C, 94.82; H, 5.18, found: C, 94.47; H, 5.03.

2.3 3,6-Diphenyl-9,9'-spirobifluorene [*m*SPh₂]



1.1 g of white solid was obtained, yield 90%; ^1H NMR (300 MHz, CD_2Cl_2) δ = 8.18 (d, $J = 1.6$ Hz, 2H), 7.92 (d, $J = 7.6$ Hz, 2H), 7.74–7.69 (m, 4H), 7.54–7.35 (m, 10H), 7.16 (t, $J = 7.5$ Hz, 2H), 6.79 (dd, $J = 7.8, 3.6$ Hz, 4H); ^{13}C NMR (75 MHz, CD_2Cl_2) δ = 148.60 (2Cqar), 148.26 (2Cqar), 142.29 (2Cqar), 141.82 (2Cqar), 141.13 (4Cqar), 128.81 (4CH), 127.88 (2CH), 127.86 (2CH), 127.37 (2CH), 127.14 (4CH), 127.10 (2CH), 124.05 (2CH), 123.84 (2CH), 120.18 (2CH), 118.84 (2CH), 65.53 (Cspiro); IR (ATR, platinum): 3034, 3022, 1599, 1565, 1476, 1448, 1432, 1396, 1283, 1255, 1184, 1155, 1118, 1075, 1011, 953, 912, 884, 869, 827, 759, 745, 737, 721, 693, 681, 646, 619, 571, 517, 501, 474, 463, 423 cm^{-1} ; HRMS (ASAP, 205 °C): Found $[\text{M}+\text{H}]^+$ 469.1950, $\text{C}_{37}\text{H}_{24}$ required 469.19508; elemental analysis calculated for $\text{C}_{37}\text{H}_{24}$: C, 94.84; H, 5.16, found: C, 94.58; H, 5.19.

2.4 3,6-diterphenyl-9,9'-spirobifluorene [*m*STPh₂]



1.8 g of white solid was obtained, yield 93%; ¹H NMR (300 MHz, CD₂Cl₂) δ = 8.32 (d, *J* = 1.7 Hz, 2H), 7.97–7.91 (m, 6H), 7.85 (t, *J* = 1.7 Hz, 2H), 7.80–7.73 (m, 8H), 7.58–7.37 (m, 16H), 7.19 (td, *J* = 7.5, 1.2 Hz, 2H), 6.89–6.82 (m, 4H); ¹³C NMR (75 MHz, CD₂Cl₂) δ = 149.07 (2Cqar), 148.98 (2Cqar), 142.83 (4Cqar), 142.80 (2Cqar), 142.72 (2Cqar), 142.31 (2Cqar), 141.53 (2Cqar), 141.47 (4Cqar), 129.29 (8CH), 128.40 (2CH), 128.36 (2CH), 128.04 (4CH), 127.81 (2CH), 127.73 (8CH), 125.59 (6CH), 124.63 (2CH), 124.31 (2CH), 120.68 (2CH), 119.61 (2CH), 66.06 (Cspiro); IR (ATR, platinum): 1596, 1575, 1496, 1474, 1447, 1409, 1389, 1076, 1031, 876, 832, 820, 761, 750, 729, 710, 698, 670, 650, 628, 614, 527, 501, 489, 420 cm⁻¹; HRMS (ASAP, 330 °C): Found [M+H]⁺ 773.3203, C₆₁H₄₀ required 773.32028; elemental analysis calculated for C₆₁H₄₀: C, 94.78; H, 5.22, found: C, 94.75, H, 5.08.

3 Structural properties

The X-ray data were collected by a Bruker AXS Kappa CCD diffractometer with Mo-Kα source ($\lambda = 0.71073 \text{ \AA}$) at 296(2) K.

Table S1. Crystal data and structure refinement for *m*SPh.

Identification code	shelx
Empirical formula	C ₃₁ H ₂₀
Formula weight	392.47
Temperature	150(2) K
Wavelength	0.71073 Å
Crystal system	monoclinic
Space group	P2 ₁ /a
Unit cell dimensions	a = 13.3029(16) Å, α = 90°.
	b = 9.8247(10) Å, β = 107.451(3)°.
	c = 16.8935(19) Å, γ = 90°.
Volume	2074.7(4) Å ³
Z	4

Density (calculated)	1.256 Mg m ⁻³
Absorption coefficient	0.071 mm ⁻¹
F(000)	824
Crystal size	0.13 x 0.09 x 0.03 mm ³
Theta range for data collection	3.167 to 27.530°.
Index ranges	-17<=h<=17, -12<=k<=11, -21<=l<=21
Reflections collected	20027
Independent reflections	4750 [R(int) = 0.0710]
Completeness to theta = 25.242°	99.2 %
Refinement method	Full-matrix least-squares on F ²
Data / restraints / parameters	4750/0/280
Goodness-of-fit on F ²	1.029
Final R indices [I>2sigma(I)]	R1 = 0.0479, wR2 = 0.1021
R indices (all data)	R1 = 0.0811, wR2 = 0.1149
Extinction coefficient	n/a
Largest diff. peak and hole	0.259 and -0.233 e Å ⁻³

Table S2. Crystal data and structure refinement for *mSPh*₂.

Identification code	shelx
Empirical formula	C37 H24
Formula weight	468.56
Temperature	293(2) K
Wavelength	0.71073 Å
Crystal system	monoclinic
Space group	P2 ₁ /a
Unit cell dimensions	a = 16.6398(11) Å α = 90°.
	b = 9.5620(6) Å, β = 106.273(4)°.
	c = 16.8786(11) Å, γ = 90°.
Volume	2578.0(3) Å ³
Z	4
Density (calculated)	1.207 Mg m ⁻³
Absorption coefficient	0.068 mm ⁻¹
F(000)	984
Crystal size	0.24 x 0.23 x 0.02 mm ³
Theta range for data collection	2.473 to 27.480°.
Index ranges	-16<=h<=21, -12<=k<=12, -21<=l<=21
Reflections collected	17443

Independent reflections	5857 [R(int) = 0.0856]
Completeness to theta = 25.242°	99.6 %
Refinement method	Full-matrix least-squares on F ²
Data / restraints / parameters	5857/0/334
Goodness-of-fit on F ²	0.967
Final R indices [I>2sigma(I)]	R1 = 0.0612, wR2 = 0.1113
R indices (all data)	R1 = 0.1906, wR2 = 0.1533
Extinction coefficient	n/a
Largest diff. peak and hole	0.168 and -0.204 e.Å ⁻³

Table S3. Crystal data and structure refinement for mSTPh.

Identification code	shelx
Empirical formula	C43 H28
Formula weight	468.56
Temperature	299(2) K
Wavelength	0.71073 Å
Crystal system	monoclinic
Space group	P2 ₁ /a
Unit cell dimensions	a = 11.2023(16) Å $\alpha = 90^\circ$.
	b = 18.855(2) Å, $\beta = 108.220(5)^\circ$.
	c = 14.855(2) Å, $\gamma = 90^\circ$.
Volume	2951.3(7) Å ³
Z	4
Density (calculated)	1.226 Mg m ⁻³
Absorption coefficient	0.069 mm ⁻¹
F(000)	1144
Crystal size	0.19 x 0.15 x 0.12 mm ³
Theta range for data collection	2.282 to 30.056°.
Index ranges	-15<=h<=15, -26<=k<=20, -20<=l<=20
Reflections collected	38725
Independent reflections	83725 [R(int) = 0.0856]
Completeness to theta = 25.242°	99.4%
Refinement method	Full-matrix least-squares on F ²
Data / restraints / parameters	8304/0/388
Goodness-of-fit on F ²	1.015
Final R indices [I>2sigma(I)]	R1 = 0.0504, wR2 = 0.1195
R indices (all data)	R1 = 0.0794, wR2 = 0.1352

Extinction coefficient	n/a
Largest diff. peak and hole	0.166 and $-0.140 \text{ e } \text{\AA}^{-3}$

4 Thermal properties

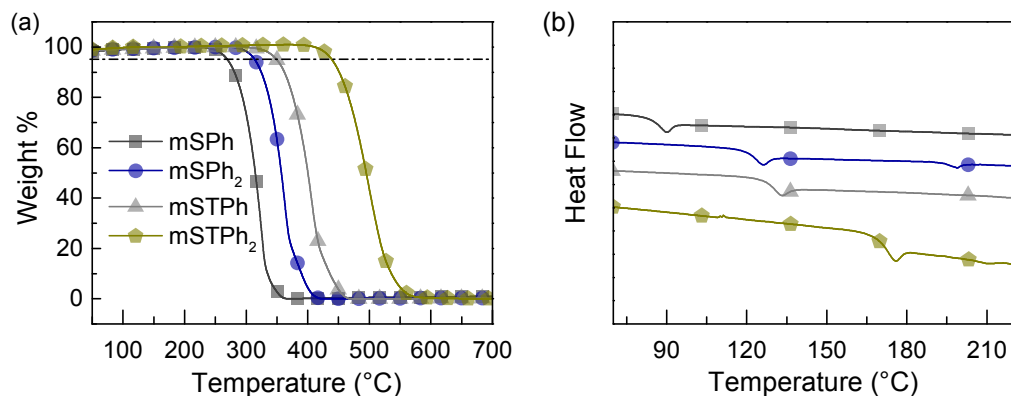


Figure S1. (a) The TGA and (b) DSC curves of **mSPh**, **mSPh₂**, **mSTPh** and **mSTPh₂**, which turns out the T_d were 262, 287, 318 and 407 °C, and the T_g were 90, 126, 133 and 175 °C for **mSPh**, **mSPh₂**, **mSTPh** and **mSTPh₂**, respectively.

5 Photophysical properties

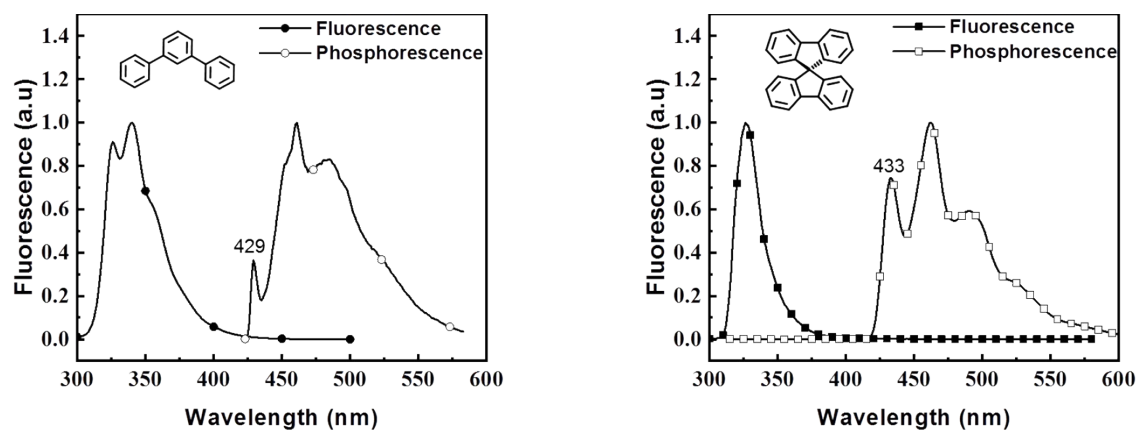


Figure S2. The PL and low temperature (77 k) phosphorescence spectra of *m*-terphenyl (left) and SBF (right) in toluene solution.

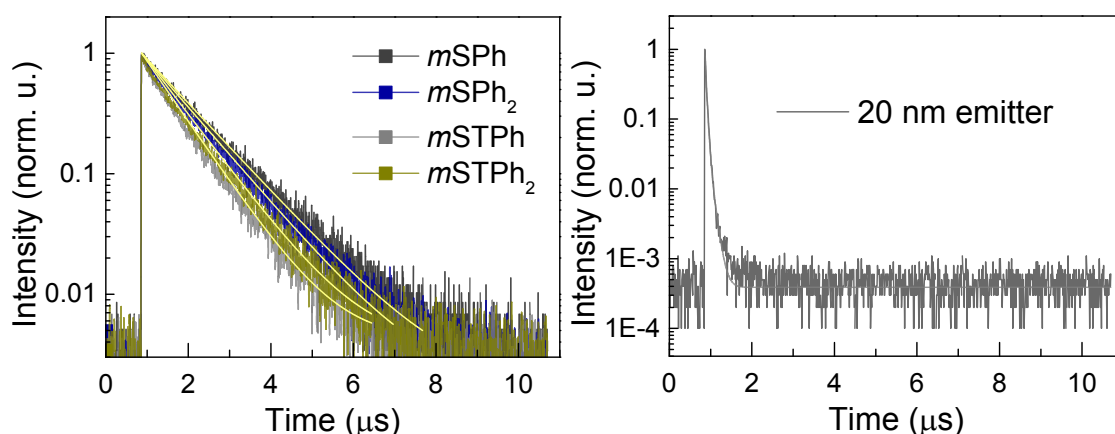


Figure S3. The transient PL curves of thin films of (left): 20 wt% of fac-Ir(ippmi)₃ doped into *mSPh*, *mSPh*₂, *mSTPh* and *mSTPh*₂, respectively, on quartz and (right): 20 nm pure emitter thin film deposited on quartz (excitation peak 373 nm).

6 Electrochemical studies

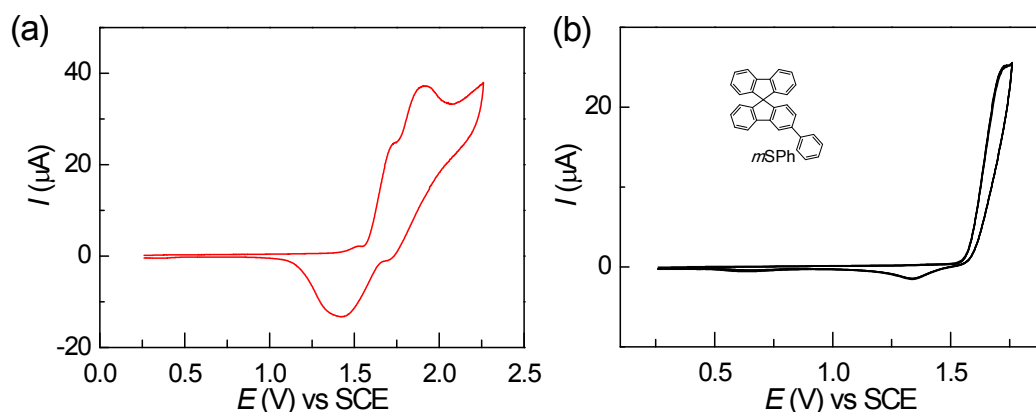


Figure S4. Cyclic voltammetry (CV) in oxidation recorded in CH₂Cl₂/[Bu₄NPF₆] 0.2 M of **mSPh** [5×10^{-3} M], platinum disk working electrode; sweep-rate: 100 mV⁻¹. (a) One cycle between 0.26 and 2.26 V. (b) One cycle between 0.22 and 1.76 V.

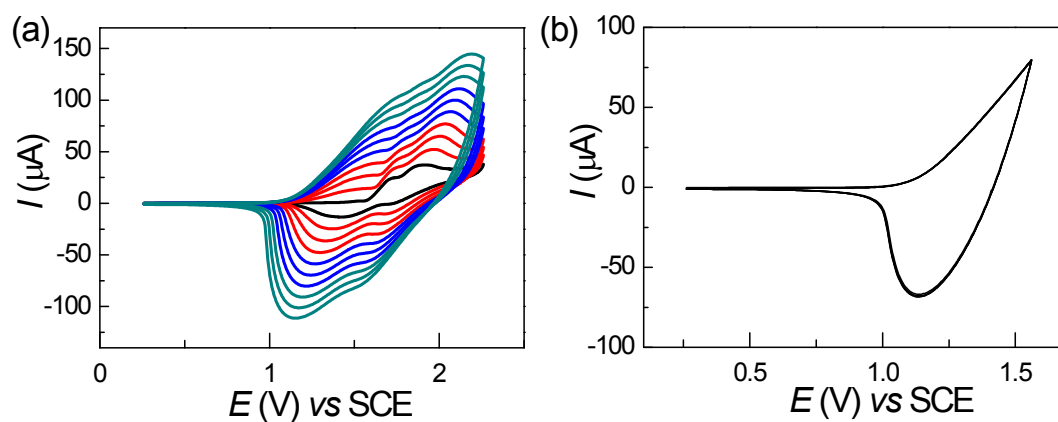


Figure S5. Cyclic voltammetry (CV) in oxidation recorded in CH₂Cl₂/[Bu₄NPF₆] 0.2 M of **mSPh** [5×10^{-3} M]. (a) Ten cycles between 0.27 and 2.27 V, platinum disk working electrode. (b) Three cycles between 0.29 and 2.1 V, platinum electrode modified in left. Sweep-rate: 100 mV⁻¹

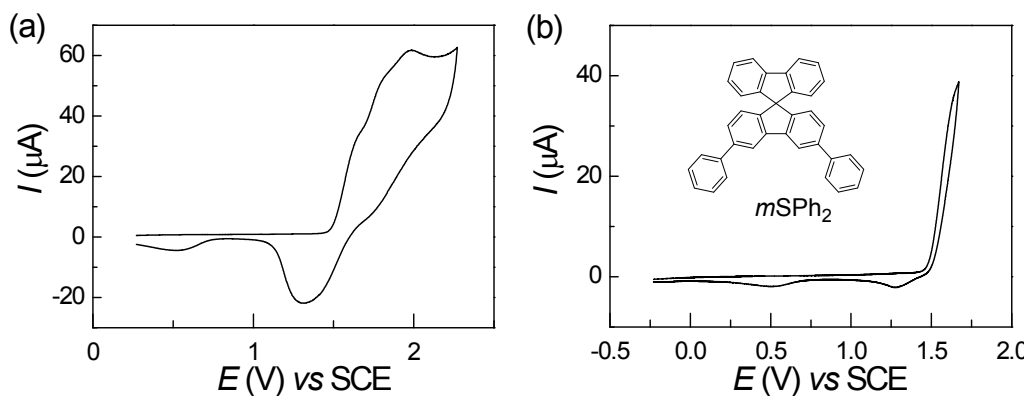


Figure S6. Cyclic voltammetry (CV) in oxidation recorded in $\text{CH}_2\text{Cl}_2/[\text{Bu}_4\text{NPF}_6]$ 0.2 M of **mSPH₂** [5×10^{-3} M], platinum disk working electrode; sweep-rate: 100 mV^{-1} . (a) One cycle between 0.3 and 2.3 V. (b) One cycle between 0.22 and 1.67 V.

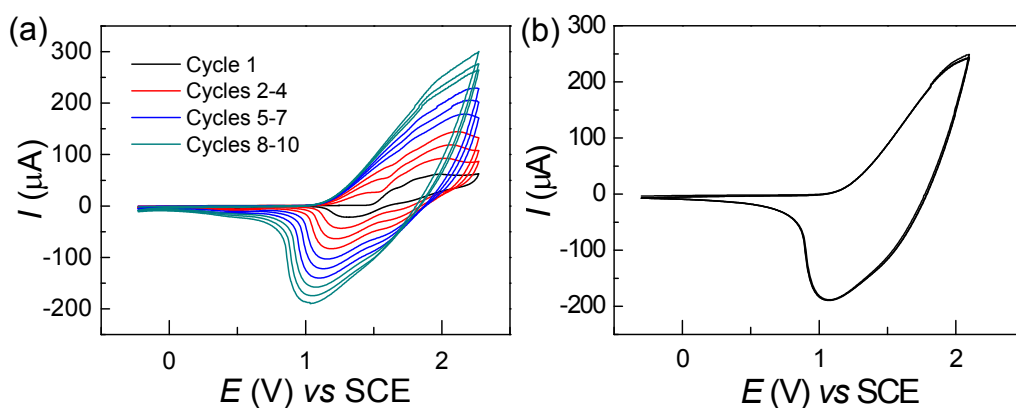


Figure S7. Cyclic voltammetry (CV) in oxidation recorded in $\text{CH}_2\text{Cl}_2/[\text{Bu}_4\text{NPF}_6]$ 0.2 M of **mSPH₂** [5×10^{-3} M]. (a) Ten cycles between 0.23 and 2.3 V, platinum disk working electrode. (b) Three cycles between -0.29 and 2.1 V, platinum electrode modified in left. Sweep-rate: 100 mV^{-1}

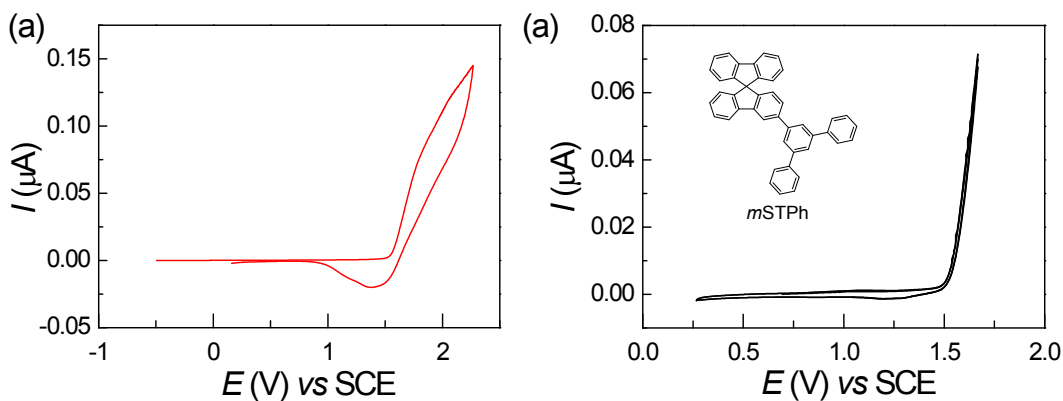


Figure S8. Cyclic voltammetry (CV) in oxidation recorded in $\text{CH}_2\text{Cl}_2/[\text{Bu}_4\text{NPF}_6]$ 0.2 M of **mSTPh** [5×10^{-3} M], platinum disk working electrode; sweep-rate: 100 mV^{-1} . (a) Three cycles between 0.26 and 1.66 V. (b) One cycle between 0.22 and 1.67 V.

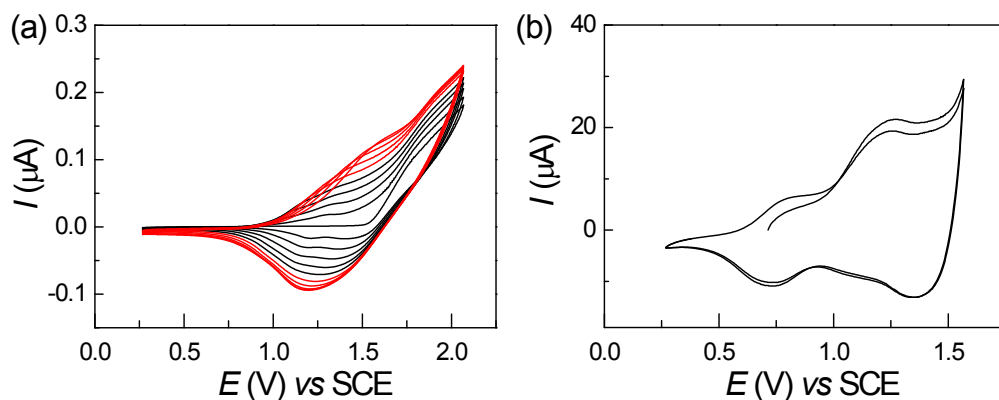


Figure S9. Cyclic voltammetry (CV) in oxidation recorded in $\text{CH}_2\text{Cl}_2/[\text{Bu}_4\text{NPF}_6]$ 0.2 M of *mSTPh* [5×10^{-3} M]. (a) Ten cycles between 0.27 and 2.07V, platinum disk working electrode. (b) Three cycle between 0.26 and 1.56 V, platinum electrode modified in left. Sweep-rate: 100 mV^{-1}

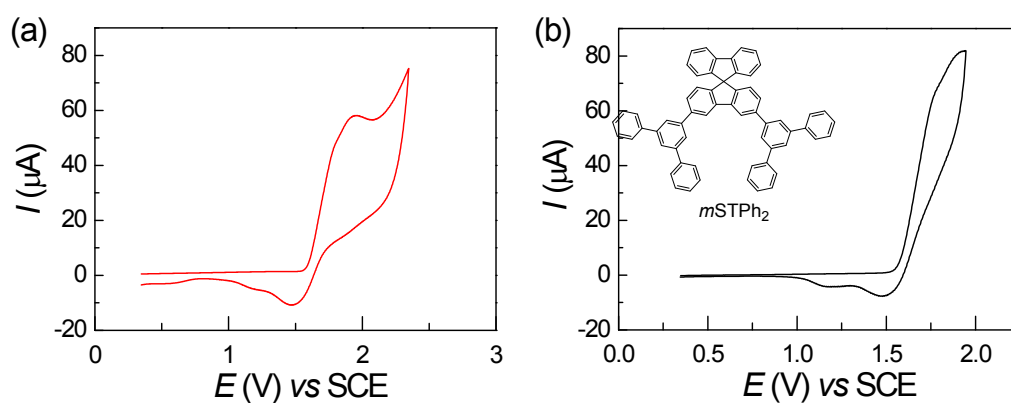


Figure S10. Cyclic voltammetry (CV) in oxidation recorded in $\text{CH}_2\text{Cl}_2/[\text{Bu}_4\text{NPF}_6]$ 0.2 M of *mSTPh*₂ [5×10^{-3} M], platinum disk working electrode; sweep-rate: 100 mV^{-1} . (a) One cycle between 0.3 and 2.3 V. (b) One cycle between 0.22 and 1.67 V.

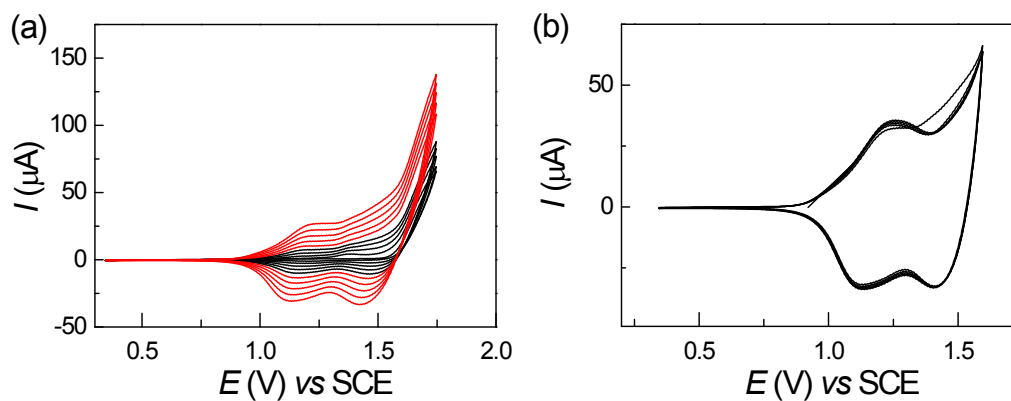


Figure S11. Cyclic voltammetry (CV) in oxidation recorded in $\text{CH}_2\text{Cl}_2/[\text{Bu}_4\text{NPF}_6]$ 0.2 M of *mSTPh*₂ [5×10^{-3} M]. (a) Ten cycles between 0.23 and 2.3 V, platinum disk working electrode. (b) Three cycle between 0.35 and 1.6 V, platinum electrode modified in left. Sweep-rate: 100 mV^{-1}

7 Molecular modelling

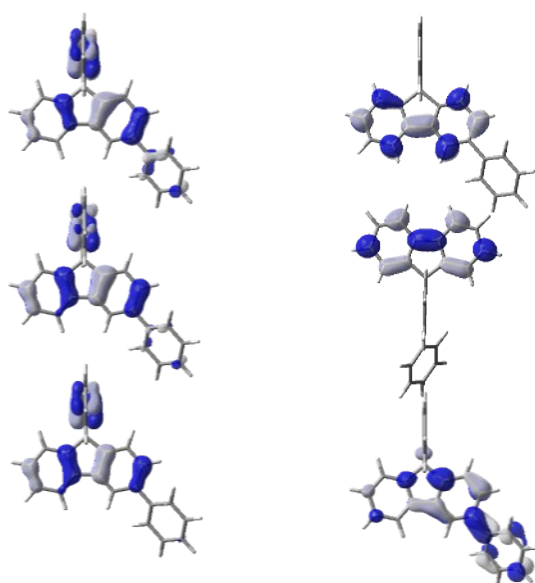


Figure S 12. The dominant natural transition orbital pairs for the first three excited singlet states of **mSPH**. The first excited state is at the top of the figure, the second at the middle and the third at the bottom; for each state, the “hole” is on the left, the “electron” on the right (td-dft, b3lyp, 6-311+g(d,p), shown with an isovalue of 0.04 [ebohr⁻³]^{1/2}).

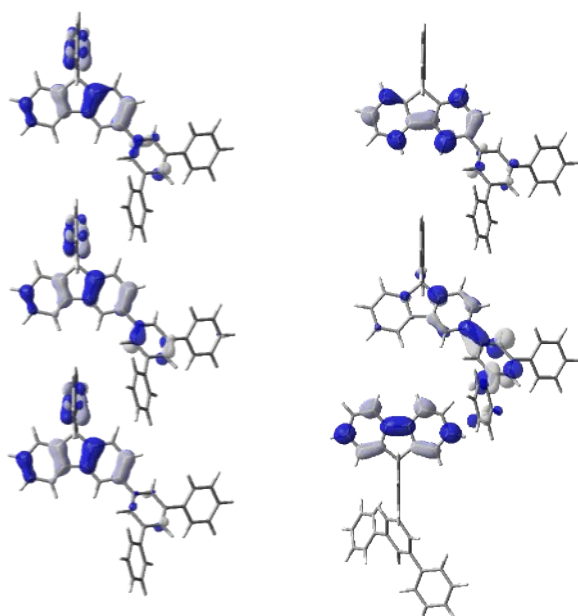


Figure S 13. The dominant natural transition orbital pairs for the first three excited singlet states of **mSTPh**. The first excited state is at the top of the figure, the second at the middle and the third at the bottom; for each state, the “hole” is on the left, the “electron” on the right (td-dft, b3lyp, 6-311+g(d,p), shown with an isovalue of 0.04 [ebohr⁻³]^{1/2}).

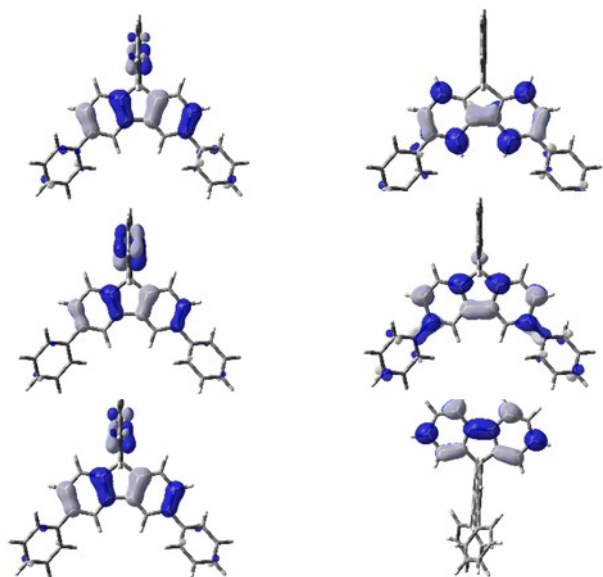


Figure S 14. The dominant natural transition orbital pairs for the first three excited singlet states of **mSPh₂**. The first excited state is at the top of the figure, the second at the middle and the third at the bottom; for each state, the “hole” is on the left, the “electron” on the right (td-dft, b3lyp, 6-311+g(d,p), shown with an isovalue of 0.04 [ebohr⁻³]^{1/2}).

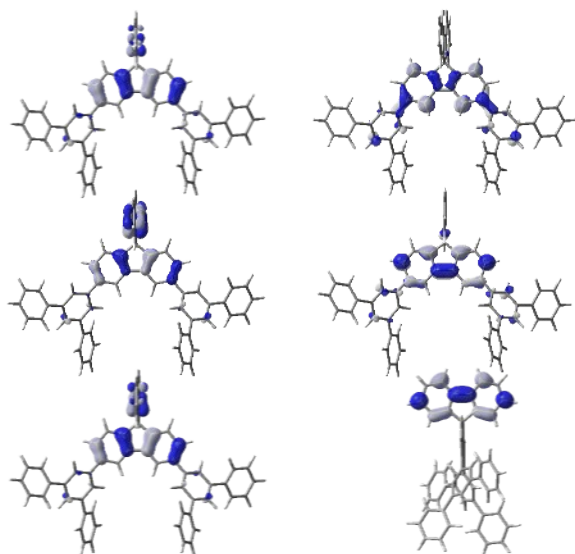


Figure S 15. The dominant natural transition orbital pairs for the first three excited singlet states of **mSTPh₂**. The first excited state is at the top of the figure, the second at the middle and the third at the bottom; for each state, the “hole” is on the left, the “electron” on the right (td-dft, b3lyp, 6-311+g(d,p), shown with an isovalue of 0.04 [ebohr⁻³]^{1/2}).

Table S4. Results of TD-DFT calculations for *mSPh* (b3lyp/6-311+g(d,p))

λ (nm)	Oscillator Strength	Major contributions	Minor contributions
306	0.089	HOMO→LUMO (42%), HOMO→L+2 (42%)	H-2→LUMO (5%), H-1→LUMO (4%), H-1→L+2 (3%)
303	0.048	HOMO→L+1 (93%)	H-1→L+3 (3%)
299	0.058	HOMO→LUMO (49%), HOMO→L+2 (42%)	H-2→LUMO (4%)
283	0.0004	HOMO→L+3 (86%)	H-3→L+1 (4%), H-1→L+3 (4%)
279	0.015	H-2→LUMO (13%), H-1→LUMO (36%), H-1→L+2 (42%)	HOMO→L+2 (4%), HOMO→L+4 (2%)
276	0.059	H-1→LUMO (51%), H-1→L+2 (36%)	HOMO→LUMO (5%), HOMO→L+2 (3%)
273	0.142	H-1→L+1 (77%)	H-3→L+1 (5%), H-3→L+3 (2%), H-2→L+1 (4%), H-1→L+3 (8%)
268	0.060	H-3→LUMO (20%), H-2→LUMO (19%), HOMO→L+4 (35%)	H-6→LUMO (3%), H-1→LUMO (4%), H-1→L+2 (5%), H-1→L+4 (4%)
264	0.101	H-1→L+1 (11%), H-1→L+3 (69%)	H-3→L+1 (3%), HOMO→L+1 (4%), HOMO→L+3 (8%)
262	0.820	H-2→LUMO (41%), HOMO→L+4 (29%)	H-2→L+2 (8%), H-1→L+2 (8%), HOMO→L+2 (6%)
260	0.019	H-2→L+1 (91%)	H-3→L+1 (2%), H-1→L+1 (3%)
259	0.049	H-2→L+2 (10%), HOMO→L+5 (41%)	H-5→LUMO (4%), H-5→L+2 (9%), H-4→L+1 (9%), H-2→L+5 (5%), H-1→L+4 (3%), H-1→L+5 (4%), HOMO→L+6 (2%)
258	0.093	H-4→L+1 (29%), H-1→L+4 (12%), HOMO→L+5 (18%)	H-5→L+2 (4%), H-3→LUMO (2%), H-2→L+2 (8%), H-2→L+5 (2%), H-1→L+6 (4%), HOMO→L+6 (8%)
254	0.005	H-2→L+2 (62%)	H-4→L+1 (9%), H-2→LUMO (4%), HOMO→L+4 (9%), HOMO→L+6 (5%)
247	0.116	H-3→LUMO (39%), HOMO→L+4 (15%)	H-4→LUMO (6%), H-4→L+1 (6%), H-2→LUMO (6%), H-2→L+2 (4%), H-2→L+4 (3%), H-1→L+2 (3%), H-1→L+4 (6%), H-1→L+6 (3%)
246	0.007	H-4→LUMO (91%)	H-3→LUMO (2%)
244	0.059	H-3→L+1 (75%)	H-6→L+1 (6%), H-3→L+2 (2%), H-1→L+1 (2%), H-1→L+3 (7%)
244	0.018	H-3→LUMO (13%), H-3→L+2 (63%), H-1→L+4 (11%)	H-3→L+1 (3%), HOMO→L+6 (2%)
243	0.013	H-2→L+3 (83%)	HOMO→L+5 (5%)
241	0.010	H-5→LUMO (12%), H-5→L+2 (17%), H-2→L+3 (10%), H-2→L+5 (25%), HOMO→L+5 (27%)	

Table S5. Results of TD-DFT calculations for *mSPh₂* (b3lyp/6-311+g(d,p))

λ (nm)	Oscillator Strength	Major contributions	Minor contributions
312	0.146	HOMO→L+1 (42%), HOMO→L+2 (44%)	H-3→LUMO (7%), H-1→LUMO (4%)
308	0.002	HOMO→LUMO (95%)	H-1→LUMO (3%)
306	0.041	HOMO→L+1 (49%), HOMO→L+2 (46%)	H-1→L+4 (2%)
290	0.032	H-2→LUMO (23%),	H-3→L+3 (3%), H-2→L+1 (5%), H-

285	0.0001	HOMO→L+3 (57%) HOMO→L+4 (88%)	2→L+2 (7%), H-1→L+3 (3%) H-1→L+4 (4%)
281	0.022	H-1→LUMO (61%), H-1→L+1 (12%), H-1→L+2 (16%)	HOMO→L+1 (3%), HOMO→L+2 (4%)
280	0.019	H-1→LUMO (30%), H-1→L+1 (26%), H-1→L+2 (32%)	H-3→LUMO (9%)
274	0.278	H-2→LUMO (22%), H-1→L+3 (13%), HOMO→L+3 (39%)	H-3→L+3 (3%), H-2→L+1 (9%), H-2→L+2 (9%)
273	0.134	H-1→L+1 (39%), H-1→L+2 (32%), H-1→L+4 (12%)	H-5→L+1 (2%), H-3→L+1 (5%), H-3→L+2 (3%)
268	0.058	H-2→L+1 (74%), H-2→L+2 (15%)	H-2→LUMO (8%)
267	0.271	H-2→LUMO (37%), H-2→L+2 (56%)	
265	0.123	H-1→L+1 (10%), H-1→L+4 (64%)	H-5→L+1 (2%), H-1→L+2 (6%), HOMO→L+4 (7%)
262	0.883	H-3→LUMO (71%)	H-2→L+3 (2%), H-1→L+1 (3%), H-1→L+2 (7%), HOMO→L+1 (3%), HOMO→L+2 (3%), HOMO→L+6 (2%)
262	0.070	H-4→L+1 (10%), H-1→L+3 (50%)	H-4→L+2 (8%), H-2→L+1 (3%), H-2→L+2 (6%), H-1→L+7 (4%), HOMO→L+5 (5%), HOMO→L+7 (4%)
260	0.021	HOMO→L+5 (58%)	H-7→LUMO (7%), H-6→L+3 (7%), H-4→L+1 (2%), H-2→L+6 (9%), H-1→L+3 (2%), H-1→L+5 (3%)
259	0.074	H-2→L+5 (11%), HOMO→L+6 (56%)	H-7→L+3 (8%), H-6→LUMO (9%), H-3→LUMO (3%), H-1→L+6 (3%)
254	0.220	H-2→L+3 (94%)	H-3→LUMO (2%)
254	0.0006	H-4→L+1 (20%), H-4→L+2 (14%), H-1→L+3 (28%), HOMO→L+7 (19%)	H-1→L+7 (9%)
253	0.060	H-3→L+1 (70%), H-3→L+2 (19%)	H-1→L+1 (2%), H-1→L+2 (2%), H-1→L+4 (2%)
252	0.043	H-3→L+1 (19%), H-3→L+2 (72%)	

Table S6. Results of TD-DFT calculations for *m*STPh (b3lyp/6-311+g(d,p))

λ (nm)	Oscillator Strength	Major contributions	Minor contributions
307	0.115	HOMO→L+1 (39%), HOMO→L+3 (41%)	H-3→LUMO (6%), H-1→LUMO (3%)
304	0.067	HOMO→LUMO (71%)	H-2→LUMO (6%), HOMO→L+3 (9%), HOMO→L+5 (2%)
303	0.047	HOMO→L+2 (90%)	H-1→L+4 (3%)
301	0.016	H-2→LUMO (13%), HOMO→LUMO (19%), HOMO→L+1 (24%), HOMO→L+3 (23%)	H-3→L+1 (4%), H-2→L+1 (3%), H-1→LUMO (5%), H-1→L+1 (2%), HOMO→L+2 (2%)
284	0.043	H-2→LUMO (30%), HOMO→L+1 (23%), HOMO→L+4 (15%)	H-3→LUMO (2%), H-3→L+1 (8%), H-3→L+3 (2%), H-2→L+1 (4%), HOMO→L+3 (8%)
282	0.010	HOMO→L+4 (69%)	H-4→L+2 (3%), H-2→LUMO (7%), H-1→L+4 (5%), HOMO→L+1 (5%)
281	0.007	H-3→LUMO (12%), H-1→L+1 (25%), H-1→L+3 (49%)	HOMO→L+3 (2%)
279	0.042	H-1→LUMO (83%)	H-1→L+5 (2%), HOMO→L+3 (7%)
273	0.135	H-1→L+2 (75%)	H-4→L+2 (6%), H-4→L+4 (2%), H-3→L+2 (5%), H-1→L+4 (8%)

273	0.151	H-2→LUMO (20%), H-2→L+1 (44%), H-2→L+3 (26%)	H-3→L+3 (2%)
271	0.221	H-3→LUMO (10%), HOMO→L+5 (59%)	H-4→L+3 (2%), H-3→L+1 (2%), HOMO→LUMO (2%), HOMO→L+3 (3%), HOMO→L+8 (6%)
271	0.528	H-3→LUMO (32%), H-2→L+3 (25%)	H-5→LUMO (2%), H-3→L+3 (7%), H-2→L+1 (3%), H-1→L+1 (9%), H-1→L+3 (4%), HOMO→L+5 (2%), HOMO→L+8 (3%)
268	0.067	H-1→L+1 (51%), H-1→L+3 (28%)	H-3→L+3 (2%), H-2→L+1 (6%), H-2→L+3 (2%), H-1→LUMO (3%)
267	0.019	H-3→LUMO (13%), H-2→L+1 (25%), H-2→L+3 (32%)	H-4→LUMO (3%), H-3→L+1 (6%), H-1→L+3 (9%), HOMO→L+8 (3%)
264	0.260	H-3→L+1 (66%), H-2→LUMO (12%)	H-2→L+3 (8%), HOMO→L+5 (5%)
263	0.077	H-3→L+2 (10%), H-1→L+4 (59%)	H-4→L+2 (2%), H-3→L+4 (2%), H-2→L+2 (2%), H-1→L+2 (6%), HOMO→L+2 (4%), HOMO→L+4 (7%)
263	0.039	H-3→L+2 (51%), H-2→L+2 (25%)	H-5→L+2 (3%), H-1→L+2 (9%), H-1→L+4 (5%)
262	0.224	H-3→LUMO (14%), H-3→L+3 (51%)	H-2→LUMO (3%), H-2→L+1 (4%), HOMO→L+5 (9%), HOMO→L+8 (2%)
261	0.004	H-3→L+2 (25%), H-2→L+2 (70%)	
259	0.002	H-6→L+2 (41%), H-1→L+8 (10%), HOMO→L+8 (19%)	H-1→L+5 (6%), H-1→L+9 (5%), HOMO→L+9 (9%)

Table S7. Results of TD-DFT calculations for *m*STPh₂ (b3lyp/6-311+g(d,p))

λ (nm)	Oscillator Strength	Major contributions	Minor contributions
314	0.210	HOMO→LUMO (25%), HOMO→L+1 (49%), HOMO→L+4 (12%)	H-5→LUMO (5%)
311	0.001	HOMO→LUMO (69%), HOMO→L+1 (19%)	H-1→LUMO (4%), HOMO→L+4 (3%)
306	0.038	HOMO→L+3 (93%)	H-1→L+6 (2%)
303	0.0005	H-3→L+5 (10%), H-2→LUMO (16%), HOMO→L+2 (55%)	H-4→L+1 (6%), H-4→L+4 (5%), H-1→L+2 (3%)
302	0.006	H-3→LUMO (15%), HOMO→L+4 (45%)	H-4→L+2 (9%), H-2→L+2 (2%), H-2→L+5 (8%), HOMO→L+1 (8%)
295	0.063	HOMO→L+5 (71%)	H-4→LUMO (6%), H-4→L+1 (6%), H-4→L+4 (3%), HOMO→L+8 (2%)
287	0.024	H-3→LUMO (24%), HOMO→L+1 (12%), HOMO→L+4 (19%), HOMO→L+6 (15%)	H-5→L+4 (2%), H-4→L+2 (6%), H-2→L+5 (8%), H-1→LUMO (4%)
286	0.041	H-3→L+5 (10%), H-2→LUMO (29%), HOMO→L+2 (40%)	H-5→L+2 (5%), H-4→L+1 (4%), H-4→L+4 (5%), HOMO→L+5 (2%)
284	0.025	H-1→LUMO (61%), HOMO→L+6 (25%)	HOMO→L+1 (2%)
283	0.021	H-1→LUMO (20%), HOMO→L+4 (13%), HOMO→L+6 (45%)	H-3→LUMO (6%), H-1→L+1 (3%), H-1→L+6 (3%)
281	0.015	H-1→L+1 (60%), H-1→L+4 (21%)	H-5→LUMO (7%), H-1→LUMO (3%)
281	0.198	H-4→LUMO (33%), H-4→L+1 (14%), HOMO→L+5 (23%)	H-5→L+5 (3%), H-4→L+4 (9%), H-2→L+1 (3%), H-1→L+5 (5%)
275	0.074	H-3→LUMO (11%), H-3→L+1	H-4→LUMO (7%), H-4→L+2 (2%), H-

		(38%), H-2→L+1 (20%)	3→L+4 (4%), H-2→LUMO (3%), H-2→L+4 (5%)
275	0.045	H-4→LUMO (12%), H-3→L+1 (24%), H-2→L+1 (33%)	H-3→LUMO (7%), H-3→L+4 (3%), H-2→LUMO (4%), H-2→L+4 (8%)
274	0.156	H-4→LUMO (27%), H-4→L+1 (39%), H-2→LUMO (18%)	H-4→L+4 (3%), H-2→L+4 (2%), H-1→L+5 (3%)
273	0.118	H-1→L+3 (69%), H-1→L+6 (12%)	H-6→L+3 (5%), H-5→L+3 (6%)
272	0.962	H-5→LUMO (31%), H-3→L+4 (24%), H-2→L+2 (19%)	H-4→L+5 (5%), H-1→L+1 (4%)
270	0.0001	H-4→L+3 (76%), H-2→L+3 (15%)	H-7→L+3 (4%)
269	0.155	H-4→L+2 (14%), H-3→LUMO (21%), H-3→L+1 (16%), H-2→L+2 (19%)	H-5→LUMO (3%), H-5→L+1 (3%), H-4→L+5 (6%), H-1→L+1 (5%), H-1→L+4 (4%), HOMO→L+7 (3%)
269	0.016	H-2→LUMO (13%), H-2→L+1 (17%), H-1→L+2 (15%), H-1→L+5 (25%)	H-4→LUMO (4%), H-4→L+1 (4%), H-4→L+3 (2%), H-4→L+4 (9%), H-3→L+5 (2%)

Table S8. Atomic coordinates of *mSPH* at the fundamental state after geometry optimization (DFT b3lyp/6-31g(d))

Atom	X (Å)	Y (Å)	Z (Å)
C	-2.10102	3.92523	-0.57806
C	-0.77307	4.3623	-0.64014
C	0.28115	3.45645	-0.50423
C	-0.01182	2.10565	-0.30543
C	-1.34904	1.66941	-0.24378
C	-2.39665	2.57227	-0.379
C	0.8696	0.9424	-0.12955
C	0.07117	-0.20455	0.03564
C	-1.41611	0.15461	-0.02002
C	2.25997	0.84648	-0.11722
C	2.87361	-0.40512	0.06271
C	2.05738	-1.54077	0.22779
C	0.66388	-1.44805	0.21426
C	-2.19181	-0.59445	-1.10891
C	-3.26303	-1.31667	-0.5493
C	-3.26592	-1.10205	0.90454
C	-2.19663	-0.24807	1.23571
C	-4.11215	-1.59199	1.90155
C	-3.87815	-1.22081	3.22743
C	-2.81409	-0.37228	3.55299
C	-1.96521	0.1199	2.55559
C	-1.95518	-0.62275	-2.47797
C	-2.80102	-1.3815	-3.29432
C	-3.86712	-2.10002	-2.7417
C	-4.10602	-2.07336	-1.36592
C	4.35436	-0.52813	0.0771
C	4.99464	-1.62424	-0.52582
C	6.38395	-1.73906	-0.51409
C	7.16583	-0.75893	0.09985
C	6.54452	0.3362	0.70286
C	5.15506	0.44942	0.69205
H	-2.91025	4.64247	-0.68565
H	-0.55994	5.41656	-0.79568
H	1.31095	3.80128	-0.55312
H	-3.42861	2.2347	-0.33179
H	2.87422	1.72923	-0.27318
H	2.52424	-2.50713	0.39499

H	0.05635	-2.33875	0.35073
H	-4.93987	-2.25176	1.65394
H	-4.52854	-1.59471	4.01376
H	-2.64486	-0.093	4.58944
H	-1.13941	0.77873	2.81074
H	-1.12784	-0.0652	-2.90901
H	-2.62816	-1.41253	-4.36671
H	-4.51535	-2.68465	-3.38912
H	-4.93525	-2.63413	-0.942
H	4.39729	-2.37914	-1.02968
H	6.85668	-2.59208	-0.99408
H	8.24881	-0.84783	0.10858
H	7.1423	1.10101	1.19199
H	4.6808	1.29175	1.18816

Table S9. Atomic coordinates of *m*SP_h at the fundamental state after geometry optimization (DFT b3lyp/6-31g(d))

Atom	X (Å)	Y (Å)	Z (Å)
C	9.9649	1.8168	12.3665
C	9.2161	0.7353	11.5768
C	9.4935	0.2257	10.3266
H	10.2532	0.4964	9.8635
C	8.6222	-0.6971	9.7715
H	8.8012	-1.0321	8.9227
C	7.4829	-1.1388	10.4483
C	7.2317	-0.6254	11.7228
H	6.4838	-0.9091	12.1972
C	8.0919	0.3041	12.2821
C	8.0076	1.0604	13.54
C	7.0677	1.0107	14.5553
H	6.3656	0.4025	14.5092
C	7.1732	1.8694	15.6436
C	8.238	2.7768	15.6765
H	8.3157	3.3573	16.399
C	9.1836	2.8342	14.6577
H	9.8835	3.4454	14.6977
C	9.0677	1.9707	13.5846
C	6.5139	-2.0616	9.8128
C	6.1794	-1.9373	8.4745
H	6.6108	-1.2989	7.9541
C	5.2158	-2.7453	7.8966
H	5.0014	-2.6435	6.9974
C	4.5789	-3.6957	8.6488
H	3.93	-4.2401	8.2649
C	4.9002	-3.8363	9.9637
H	4.4713	-4.4845	10.4739
C	5.85	-3.0331	10.5479
H	6.0511	-3.1432	11.4494
C	6.162	1.8273	16.7325
C	4.8222	1.6322	16.4545
H	4.5439	1.5581	15.5702
C	3.8884	1.5462	17.4727
H	2.9923	1.403	17.2703
C	4.2852	1.6724	18.7867
H	3.6607	1.604	19.4713
C	5.6015	1.899	19.077
H	5.8679	2.0101	19.9611
C	6.5353	1.964	18.0671
H	7.4296	2.1012	18.2798

C	11.3902	1.3951	12.7297
C	11.8006	0.3767	13.5522
H	11.1772	-0.1642	13.9805
C	13.1658	0.1654	13.7364
H	13.4605	-0.5195	14.2929
C	14.0852	0.9763	13.0899
H	14.9945	0.825	13.2122
C	13.6728	2.0013	12.2722
H	14.2989	2.5327	11.8363
C	12.3129	2.2366	12.1004
C	11.5944	3.2664	11.3605
C	12.0444	4.345	10.5952
H	12.9553	4.4881	10.473
C	11.1226	5.1912	10.0249
H	11.4161	5.9111	9.515
C	9.7692	4.9875	10.1981
H	9.1615	5.5711	9.8048
C	9.306	3.9185	10.9549
H	8.3938	3.7792	11.0713
C	10.2275	3.0675	11.5304

Table S10. Atomic coordinates of *m*STPh at the fundamental state after geometry optimization (DFT b3lyp/6-31g(d))

Atom	X (Å)	Y (Å)	Z (Å)
C	-3.66185	-0.1237	-0.10685
C	-2.1551	0.09131	0.06035
C	-1.48709	1.08245	0.76826
H	-2.0388	1.84328	1.31397
C	-0.09048	1.08437	0.78047
H	0.43534	1.84162	1.3548
C	0.65378	0.10766	0.09143
C	-0.03515	-0.88823	-0.6217
H	0.52351	-1.6332	-1.18175
C	-1.42897	-0.89373	-0.63427
C	-2.3804	-1.79894	-1.29467
C	-2.17069	-2.92192	-2.09776
H	-1.16399	-3.25955	-2.33072
C	-3.2786	-3.60795	-2.59998
C	-4.57727	-3.17859	-2.30411
H	-5.42899	-3.72325	-2.70256
C	-4.78938	-2.05369	-1.49968
H	-5.79869	-1.72174	-1.27125
C	-3.68825	-1.36928	-0.99939
C	2.14019	0.13043	0.12001
C	2.84048	1.34332	0.04847
H	2.28582	2.26953	-0.06712
C	4.24226	1.38062	0.05687
C	4.94427	0.16937	0.13764
H	6.02821	0.18762	0.19815
C	4.27514	-1.06089	0.20902
C	2.87316	-1.06212	0.19975
H	2.3428	-2.00794	0.25549
C	-4.41038	-0.29887	1.21889
C	-4.1994	-1.24446	2.21507
H	-3.41784	-1.99263	2.11229
C	-5.01096	-1.21809	3.35452
H	-4.85737	-1.95144	4.14156
C	-6.01808	-0.25586	3.4889
H	-6.64017	-0.24851	4.38

C	-6.23157	0.69525	2.48875
H	-7.01547	1.44042	2.59832
C	-5.42267	0.67074	1.35064
C	-5.41194	1.5267	0.15611
C	-6.20735	2.61922	-0.1959
H	-6.99615	2.96919	0.46524
C	-5.9738	3.25875	-1.41529
H	-6.58521	4.11026	-1.70204
C	-4.96018	2.81359	-2.27126
H	-4.7909	3.32184	-3.2167
C	-4.1621	1.71917	-1.92057
H	-3.37543	1.37478	-2.58666
C	-4.39314	1.08154	-0.70767
C	5.03503	-2.3345	0.31107
C	4.58713	-3.38043	1.13552
C	6.22177	-2.52601	-0.41638
C	5.29957	-4.57523	1.2284
H	3.68667	-3.2444	1.72805
C	6.93535	-3.72002	-0.32329
H	6.57322	-1.74002	-1.07916
C	6.47721	-4.75062	0.49948
H	4.93813	-5.36726	1.87913
H	7.84673	-3.84827	-0.90154
H	7.03294	-5.68159	0.57218
C	4.968	2.67564	-0.0182
C	4.48956	3.81194	0.65572
C	6.1519	2.79825	-0.76494
C	5.16944	5.02697	0.58524
H	3.59015	3.7338	1.26019
C	6.83337	4.01241	-0.83491
H	6.52622	1.93953	-1.31533
C	6.345	5.13279	-0.16026
H	4.78435	5.89042	1.12149
H	7.74304	4.08518	-1.42534
H	6.87556	6.07954	-0.21496
H	-3.1306	-4.48343	-3.22661

Table S11. Atomic coordinates of *m*STPh₂ at the fundamental state after geometry optimization (DFT b3lyp/6-31g(d))

Atom	X (Å)	Y (Å)	Z (Å)
C	0.000001	3.782188	-0.000017
C	-1.174764	2.80969	-0.139058
C	-2.526725	3.089428	-0.293152
H	-2.879866	4.116128	-0.340005
C	-3.431312	2.030705	-0.399506
H	-4.485809	2.245053	-0.547308
C	-3.005348	0.689369	-0.351946
C	-1.634979	0.420986	-0.193951
H	-1.292007	-0.607964	-0.127832
C	-0.729753	1.475686	-0.089301
C	0.729741	1.475679	0.089324
C	1.634956	0.420971	0.19399
H	1.291971	-0.607977	0.127918
C	3.005333	0.689343	0.351943
C	3.431314	2.030674	0.39945
H	4.485817	2.245016	0.547218
C	2.526737	3.089406	0.293085
H	2.879893	4.116102	0.339896
C	1.174771	2.809679	0.139032

C	-3.988262	-0.420208	-0.468236
C	-5.239735	-0.338123	0.159139
H	-5.472358	0.531393	0.766365
C	-6.171081	-1.382945	0.073375
C	-5.827327	-2.528378	-0.658957
H	-6.559312	-3.321549	-0.777259
C	-4.584054	-2.643349	-1.297274
C	-3.676564	-1.579811	-1.192023
H	-2.710559	-1.655767	-1.681979
C	3.988233	-0.420246	0.468234
C	3.676543	-1.579827	1.192062
H	2.710558	-1.655765	1.682061
C	4.584027	-2.643371	1.297302
C	5.827287	-2.528433	0.65895
H	6.559258	-3.321619	0.777238
C	6.171025	-1.38302	-0.073417
C	5.23969	-0.338193	-0.159183
H	5.472317	0.531314	-0.766418
C	0.139715	4.753929	-1.176934
C	0.300153	4.463539	-2.526368
H	0.341036	3.433503	-2.870617
C	0.408387	5.520624	-3.436611
H	0.53413	5.308549	-4.494913
C	0.356043	6.8477	-2.995719
H	0.441547	7.657725	-3.715188
C	0.19496	7.141364	-1.639876
H	0.154993	8.174141	-1.302948
C	0.086722	6.087841	-0.729639
C	-0.086515	6.087823	0.729693
C	-0.194655	7.141325	1.639967
H	-0.154568	8.17411	1.303077
C	-0.355797	6.847628	2.995796
H	-0.441229	7.657637	3.715293
C	-0.408298	5.520542	3.436637
H	-0.534095	5.308442	4.494928
C	-0.300156	4.463478	2.526358
H	-0.341164	3.433435	2.870568
C	-0.139655	4.753902	1.17694
C	7.493346	-1.278621	-0.744213
C	8.194067	-0.061101	-0.774184
C	8.078014	-2.39454	-1.366436
C	9.433893	0.037674	-1.403905
H	7.77313	0.808465	-0.277079
C	9.318438	-2.297243	-1.995223
H	7.542319	-3.339721	-1.3781
C	10.00216	-1.080295	-2.017205
H	9.960925	0.988262	-1.407385
H	9.747269	-3.172263	-2.476737
H	10.968809	-1.003879	-2.507671
C	4.243082	-3.857751	2.08405
C	3.530427	-3.761468	3.291139
C	4.624283	-5.134998	1.639644
C	3.209431	-4.901369	4.026853
H	3.248759	-2.782078	3.667784
C	4.304661	-6.275268	2.375259
H	5.153983	-5.234949	0.696262
C	3.595232	-6.16371	3.572413
H	2.664259	-4.801647	4.961841
H	4.603048	-7.253584	2.007456
H	3.345382	-7.052265	4.14587
C	-4.243098	-3.85775	-2.083981

C	-3.530499	-3.761503	-3.291107
C	-4.624251	-5.134991	-1.639515
C	-3.209501	-4.901427	-4.026785
H	-3.24888	-2.782127	-3.667819
C	-4.304628	-6.275284	-2.375092
H	-5.153912	-5.234925	-0.696109
C	-3.595247	-6.163761	-3.572278
H	-2.664369	-4.801726	-4.961798
H	-4.602982	-7.253591	-2.007236
H	-3.345397	-7.052333	-4.145708
C	-7.493417	-1.27852	0.744132
C	-8.194065	-0.060957	0.774184
C	-8.078183	-2.394457	1.366239
C	-9.433903	0.037844	1.403871
H	-7.773068	0.808619	0.277152
C	-9.318623	-2.297136	1.994983
H	-7.542541	-3.339667	1.377861
C	-10.002265	-1.080145	2.017049
H	-9.960883	0.98846	1.407421
H	-9.747538	-3.172165	2.476408
H	-10.968928	-1.00371	2.507485

Table S12. Atomic coordinates of *mSPh* at the first triplet state after geometry optimization (TD-DFT b3lyp/6-31+g(d))

Atom	X (Å)	Y (Å)	Z (Å)
C	-2.051804	3.951125	-0.559706
C	-0.691538	4.382134	-0.605151
C	0.348079	3.488649	-0.471223
C	0.048444	2.089588	-0.280966
C	-1.348653	1.665753	-0.235535
C	-2.366553	2.579437	-0.373336
C	0.877811	0.980859	-0.119315
C	0.047684	-0.225907	0.034168
C	-1.437831	0.147187	-0.021738
C	2.309486	0.858051	-0.099574
C	2.900371	-0.380611	0.064893
C	2.052661	-1.554593	0.215728
C	0.639523	-1.454456	0.19561
C	-2.2229	-0.587322	-1.113624
C	-3.302236	-1.302755	-0.558413
C	-3.302664	-1.096075	0.89718
C	-2.223608	-0.254271	1.23176
C	-4.15498	-1.582535	1.892887
C	-3.916271	-1.219728	3.222031
C	-2.841687	-0.382633	3.551892
C	-1.987727	0.105588	2.554811
C	-1.986891	-0.608984	-2.484595
C	-2.841133	-1.354152	-3.307204
C	-3.915748	-2.066659	-2.757801
C	-4.154392	-2.046401	-1.380159
C	4.372515	-0.534026	0.080471
C	4.989711	-1.682236	-0.45581
C	6.378472	-1.818201	-0.45996
C	7.187912	-0.815326	0.081679
C	6.591441	0.326332	0.628025
C	5.203985	0.463573	0.629248
H	-2.850254	4.679064	-0.668201
H	-0.479056	5.438747	-0.749143
H	1.380319	3.826378	-0.508026

H	-3.406434	2.262643	-0.340364
H	2.923063	1.741088	-0.254741
H	2.515168	-2.519958	0.3913
H	0.037963	-2.352544	0.316456
H	-4.990454	-2.232504	1.64373
H	-4.570357	-1.590623	4.007193
H	-2.669617	-0.109985	4.589997
H	-1.155323	0.755394	2.81416
H	-1.154274	-0.0567	-2.91374
H	-2.66943	-1.379881	-4.380264
H	-4.570183	-2.640615	-3.409092
H	-4.989964	-2.601894	-0.960785
H	4.378169	-2.46212	-0.90108
H	6.829187	-2.708509	-0.891696
H	8.269355	-0.924122	0.084089
H	7.208748	1.106699	1.066429
H	4.754513	1.341012	1.086134

Table S13 Atomic coordinates of *m*SPh₂ at the first triplet state after geometry optimization (TD-DFT b3lyp/6-31+g(d))

Atom	X (Å)	Y (Å)	Z (Å)
C	0.00208	1.77379	-0.00002
C	1.18206	0.79457	0.03102
C	2.5328	1.05356	0.06034
H	2.90422	2.07571	0.07447
C	3.45091	-0.02149	0.08216
H	4.51361	0.18735	0.14752
C	3.00272	-1.39943	0.07257
C	1.64484	-1.66557	0.04199
H	1.29004	-2.69143	-0.00406
C	0.69734	-0.58846	0.02199
C	-0.69883	-0.58679	-0.02194
C	-1.6489	-1.66164	-0.04191
H	-1.29655	-2.68833	0.00434
C	-3.00614	-1.39228	-0.07268
C	-3.45104	-0.01322	-0.08251
H	-4.51322	0.19817	-0.14805
C	-2.53035	1.05964	-0.06069
H	-2.89934	2.08267	-0.07501
C	-1.18024	0.79743	-0.03113
C	3.99919	-2.49613	0.088
C	5.22813	-2.37008	-0.58934
H	5.44381	-1.46136	-1.1447
C	6.15959	-3.40924	-0.59014
H	7.09541	-3.29101	-1.13093
C	5.89089	-4.59843	0.09391
H	6.61861	-5.40579	0.09781
C	4.67931	-4.73656	0.77924
H	4.46445	-5.6507	1.32733
C	3.7475	-3.69881	0.77764
H	2.82422	-3.80823	1.34017
C	-4.00522	-2.48658	-0.08807
C	-3.75621	-3.69007	-0.77729
H	-2.83303	-3.80187	-1.33952
C	-4.69048	-4.7256	-0.77884
H	-4.47764	-5.6404	-1.3266
C	-5.90193	-4.58439	-0.09389
H	-6.63157	-5.39	-0.09777
C	-6.16798	-3.39436	0.58975

H	-7.10365	-3.27375	1.13025
C	-5.23405	-2.35742	0.58889
H	-5.44772	-1.44803	1.14394
C	-0.0274	2.74674	1.18408
C	-0.0629	2.4553	2.54408
H	-0.07278	1.42485	2.89129
C	-0.0855	3.51232	3.46275
H	-0.113	3.29998	4.52846
C	-0.07265	4.84165	3.01891
H	-0.09044	5.65136	3.74411
C	-0.03697	5.13661	1.65251
H	-0.02703	6.17042	1.31528
C	-0.01422	4.08207	0.73494
C	0.02421	4.08209	-0.73475
C	0.04962	5.13666	-1.65221
H	0.04232	6.17046	-1.31488
C	0.08451	4.84175	-3.01864
H	0.10433	5.65148	-3.74377
C	0.09397	3.51243	-3.46262
H	0.12087	3.30013	-4.52836
C	0.06871	2.45539	-2.54406
H	0.07596	1.42495	-2.89137
C	0.03399	2.74678	-1.18402

Table S14 Atomic coordinates of *m*STPh at the first triplet state after geometry optimization (TD-DFT b3lyp/6-31+g(d))

Atom	X (Å)	Y (Å)	Z (Å)
C	-3.690204	-0.134402	-0.095484
C	-2.1841	0.098438	0.067142
C	-1.51522	1.125855	0.686114
H	-2.058363	1.935936	1.167586
C	-0.098761	1.128424	0.706308
H	0.424019	1.918299	1.234837
C	0.672896	0.062988	0.082235
C	0.004188	-0.972523	-0.54337
H	0.55983	-1.755728	-1.051338
C	-1.431945	-0.993514	-0.573627
C	-2.330203	-1.89573	-1.142518
C	-2.119374	-3.11647	-1.882245
H	-1.110518	-3.470011	-2.077439
C	-3.213465	-3.820261	-2.33509
C	-4.543573	-3.365651	-2.086672
H	-5.386386	-3.942237	-2.456015
C	-4.771039	-2.167191	-1.361265
H	-5.788735	-1.830185	-1.178327
C	-3.697166	-1.444757	-0.896867
C	2.152249	0.112202	0.119907
C	2.834405	1.341153	0.061496
H	2.267082	2.261716	-0.037589
C	4.235727	1.402119	0.05373
C	4.962631	0.203041	0.11957
H	6.0469	0.240924	0.173324
C	4.313666	-1.041028	0.193212
C	2.912942	-1.068789	0.193632
H	2.402826	-2.025358	0.256059
C	-4.44915	-0.218026	1.233811
C	-4.240754	-1.090296	2.297462
H	-3.455304	-1.841086	2.254697
C	-5.060962	-0.987574	3.42819

H	-4.909965	-1.66243	4.266863
C	-6.074921	-0.021833	3.486892
H	-6.703453	0.045579	4.371349
C	-6.286048	0.85558	2.418793
H	-7.074889	1.602305	2.47079
C	-5.467712	0.7537	1.289894
C	-5.452325	1.522088	0.036615
C	-6.251106	2.583598	-0.398867
H	-7.046802	2.977598	0.22899
C	-6.011178	3.135112	-1.661202
H	-6.624278	3.960968	-2.013251
C	-4.98805	2.633457	-2.477201
H	-4.814556	3.073163	-3.456044
C	-4.187368	1.570008	-2.041589
H	-3.394484	1.182797	-2.677064
C	-4.424521	1.019946	-0.78582
C	4.938256	2.711717	-0.017796
C	4.474318	3.822358	0.709229
C	6.085602	2.873405	-0.81452
C	5.133532	5.051188	0.642324
H	3.604251	3.714974	1.351817
C	6.746043	4.101528	-0.882478
H	6.448721	2.035945	-1.404709
C	6.272889	5.196665	-0.154166
H	4.761079	5.893373	1.220389
H	7.626345	4.204629	-1.512255
H	6.786589	6.153152	-0.20661
C	5.098159	-2.301543	0.292076
C	4.697051	-3.338418	1.153221
C	6.261839	-2.489156	-0.474748
C	5.432773	-4.521511	1.243949
H	3.81561	-3.206045	1.775324
C	6.99854	-3.671681	-0.384953
H	6.57855	-1.711197	-1.164712
C	6.587251	-4.693909	0.475044
H	5.108117	-5.30565	1.923576
H	7.890423	-3.797215	-0.994033
H	7.160622	-5.61465	0.545772
H	-3.068105	-4.741418	-2.894205

Table S15 Atomic coordinates of *m*STPh₂ at the first triplet state after geometry optimization (TD-DFT b3lyp/6-31+g(d))

Atom	X (Å)	Y (Å)	Z (Å)
C	-0.00008	3.81596	-0.00044
C	1.17398	2.83827	0.13237
C	2.51681	3.09888	0.27872
H	2.8845	4.12143	0.32538
C	3.43105	2.02502	0.37897
H	4.48384	2.23547	0.53552
C	2.98682	0.64683	0.33005
C	1.63696	0.37872	0.18286
H	1.28829	-0.64747	0.10677
C	0.69378	1.45485	0.08146
C	-0.69383	1.4548	-0.08181
C	-1.63697	0.3786	-0.18295
H	-1.28827	-0.64755	-0.10651
C	-2.98683	0.64662	-0.33035
C	-3.4311	2.02479	-0.37978
H	-4.48387	2.23515	-0.53653

C	-2.51691	3.09871	-0.27976
H	-2.88463	4.12123	-0.3268
C	-1.17408	2.8382	-0.13316
C	3.9803	-0.44952	0.42977
C	5.25755	-0.31692	-0.14214
H	5.52033	0.60421	-0.65359
C	6.20225	-1.35136	-0.07355
C	5.8549	-2.53626	0.59339
H	6.57993	-3.34247	0.65832
C	4.59162	-2.69847	1.18494
C	3.66829	-1.64773	1.09546
H	2.69028	-1.76135	1.55355
C	-3.98025	-0.44979	-0.42981
C	-3.66814	-1.64822	-1.09507
H	-2.69008	-1.76198	-1.55303
C	-4.59143	-2.69901	-1.18428
C	-5.85478	-2.53664	-0.59291
H	-6.57975	-3.34292	-0.65766
C	-6.20223	-1.35153	0.0736
C	-5.25756	-0.31705	0.14193
H	-5.52041	0.60425	0.65303
C	-0.13234	4.78892	1.17664
C	-0.28373	4.49756	2.52864
H	-0.32184	3.4671	2.87392
C	-0.3863	5.55462	3.44181
H	-0.50464	5.34239	4.50131
C	-0.33713	6.88395	3.00043
H	-0.41796	7.6937	3.72128
C	-0.18483	7.17881	1.64208
H	-0.14714	8.21259	1.30672
C	-0.08231	6.12422	0.73006
C	0.082	6.12422	-0.73093
C	0.18446	7.17882	-1.64295
H	0.1467	8.21259	-1.30759
C	0.33677	6.88397	-3.0013
H	0.41756	7.69372	-3.72215
C	0.38604	5.55465	-3.44268
H	0.5044	5.34242	-4.50218
C	0.28353	4.49758	-2.52951
H	0.32171	3.46712	-2.87479
C	0.13212	4.78893	-1.1775
C	-7.54715	-1.19333	0.6908
C	-8.70187	-1.65707	0.03577
C	-7.69845	-0.57597	1.94517
C	-9.96383	-1.50911	0.61441
H	-8.6125	-2.11534	-0.94582
C	-8.95997	-0.42725	2.52468
H	-6.81801	-0.2316	2.48163
C	-10.09892	-0.8933	1.86191
H	-10.84327	-1.86776	0.08514
H	-9.05139	0.04582	3.49936
H	-11.08125	-0.77779	2.31272
C	-4.24205	-3.95972	-1.89362
C	-3.52525	-3.93383	-3.10313
C	-4.61993	-5.20994	-1.37253
C	-3.19708	-5.11655	-3.7685
H	-3.24381	-2.97814	-3.53788
C	-4.29247	-6.39329	-2.03717
H	-5.15325	-5.25616	-0.42649
C	-3.57929	-6.35219	-3.23857
H	-2.6493	-5.07137	-4.70659

H	-4.58751	-7.34882	-1.61048
H	-3.32384	-7.27324	-3.75618
C	4.24233	-3.95894	1.89473
C	3.52555	-3.93268	3.10425
C	4.62029	-5.20933	1.37409
C	3.19747	-5.11519	3.77004
H	3.24405	-2.97686	3.53867
C	4.29292	-6.39246	2.03915
H	5.1536	-5.25587	0.42805
C	3.57976	-6.35099	3.24055
H	2.64969	-5.06971	4.70812
H	4.58803	-7.34813	1.6128
H	3.32437	-7.27188	3.75849
C	7.5471	-1.19333	-0.69094
C	8.70191	-1.65667	-0.03577
C	7.69824	-0.57655	-1.94561
C	9.96381	-1.50887	-0.61458
H	8.61264	-2.11448	0.94604
C	8.9597	-0.42799	-2.52528
H	6.81772	-0.2325	-2.48214
C	10.09874	-0.89363	-1.86239
H	10.84333	-1.86719	-0.08523
H	9.05102	0.04463	-3.5002
H	11.08103	-0.77825	-2.31333

8 Charge Transport

Space-charged limited current (SCLC) diodes

The hole-only device (HOD) has a configuration of ITO/HAT-CN (10 nm)/Host (100 nm)/HATCN (10 nm)/ Al (120 nm), and electron-only device (EOD) is ITO/Liq (4 nm)/Host (100 nm)/Liq (4 nm)/Al (120 nm). After the fabrication, the devices were encapsulated before testing in dark.

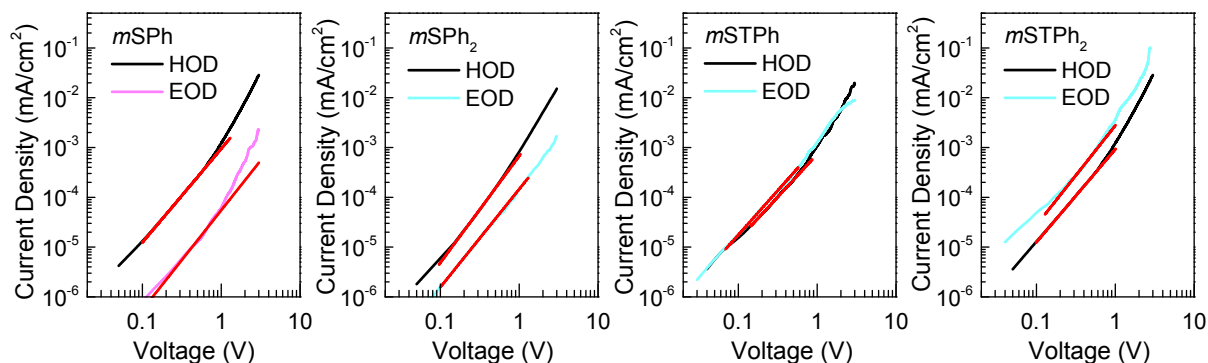


Figure S16. The J - V curves of hole-only (HOD) and electron-only devices using $mSPh$, $mSPh_2$, $mSTPh$ and $mSTPh_2$, respectively.

The J - V curves of charge-only devices show the charge transport ability of the compounds. Based on the Schottky thermionic region and space-charge-limited current (SCLC) model, the curves can be divided into two parts under low bias. We assign the second region of the J - V curve as assigned as the SCLC region, which then can be described by an equation:

$$J = \frac{9}{8} \epsilon \epsilon_0 \mu_0 \exp\left(\frac{\beta}{L}\right) \frac{\sqrt{V} V^2}{L^3}$$

in which V is the driving voltage, L is the thickness of the thin layer, ϵ_0 the permittivity of the free space, ϵ is the relative dielectric constant (estimated to be 3.0 here), μ_0 is the zero-field mobility and β is Poole-Frenkel factor. The thickness L equals to 100 nm, the zero-field mobility of the compounds was calculated and summarized Table 1.

9 Phosphorescent OLED characteristics

The architecture of the devices is the following: ...

Blue PhOLEDs: ITO/HAT-CN (10 nm)/TAPC (35 nm)/TCTA (8 nm)/host: 15 wt% fac-Ir(iprpmi)₃, 20 nm)/TmPyPB (40 nm)/Liq (2nm)/Al (120 nm).

Green PhOLEDs: ITO/HAT-CN (10 nm)/TAPC (40 nm)/TCTA (8 nm)/host: 14 wt% Ir(ppy)₂acac, 20 nm/TmPyPB (45 nm)/Liq (2nm)/Al (120 nm).

Red PhOLEDs: ITO/HAT-CN (10 nm)/TAPC (45 nm)/TCTA (8 nm)/host: 12 wt% Ir(MDQ)₂acac, 20 nm/TmPyPB (55 nm)/Liq (2nm)/Al (120 nm).

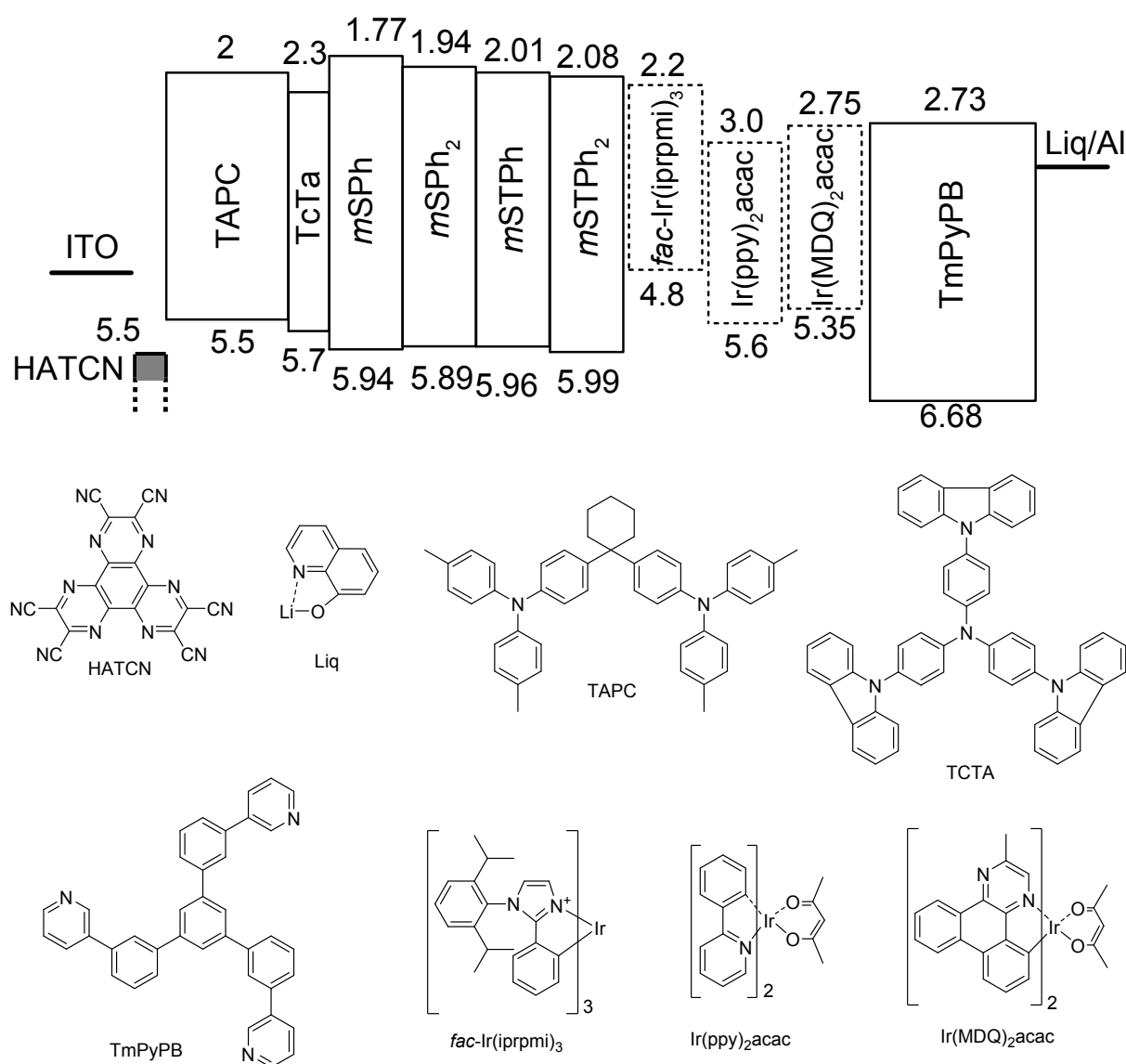


Figure S17. The energy level alignment of the device and the molecular structures of materials in different layers. The LUMO/HOMO values of hosts were taken from the CV measurements and other material were taken from literature.

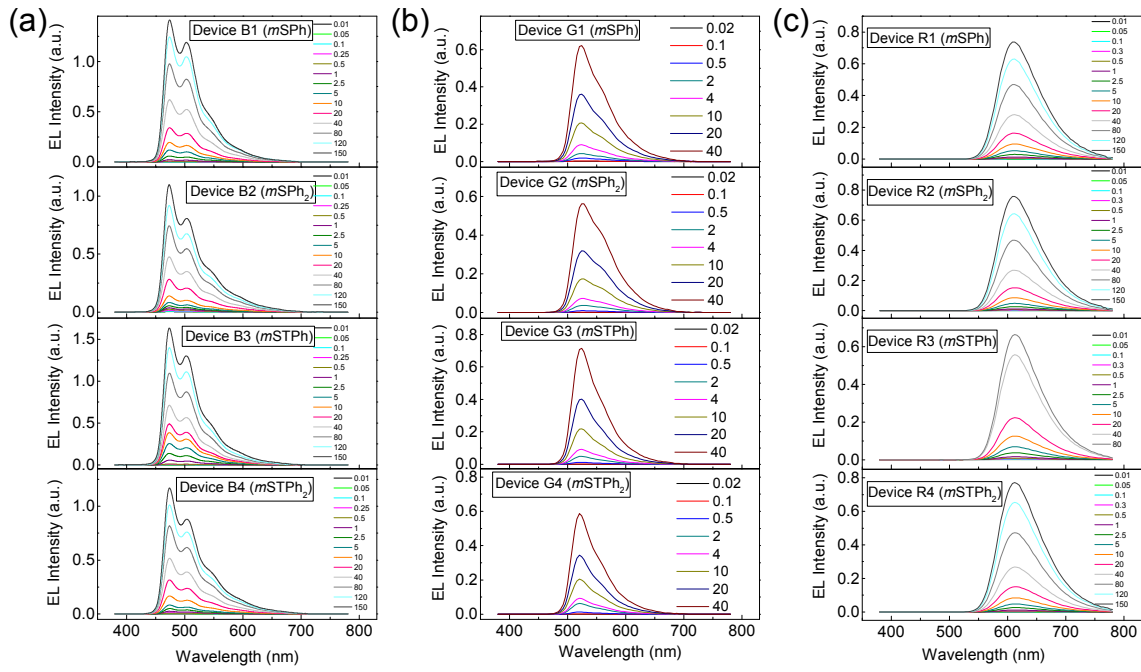


Figure S18. The EL spectrum of (a) blue (B1–4), (b) green (G1–4) and (c) red (R1–4) PhOLEDs using *m*SPh, *m*SPh₂, *m*STPh and *m*STPh₂, respectively. The legends show the driving current densities of each spectrum.

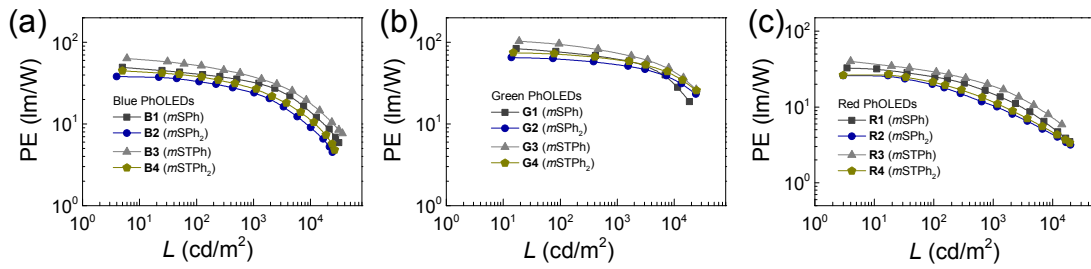


Figure S19 The PE–*L* curves of (a) blue (B1–4), (b) green (G1–4) and (c) red (R1–4) PhOLEDs using *m*SPh, *m*SPh₂, *m*STPh and *m*STPh₂, respectively.

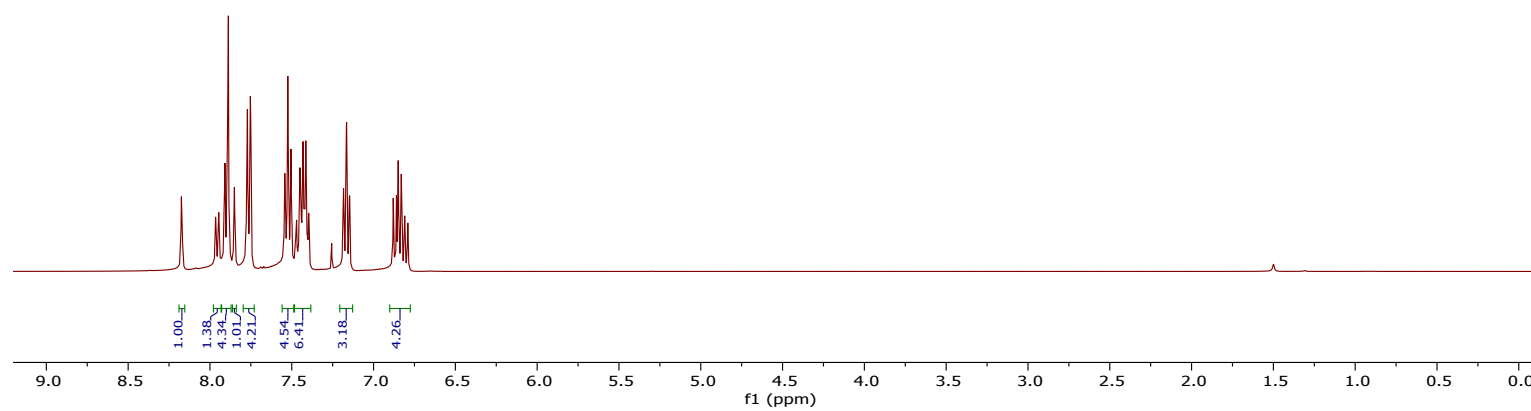
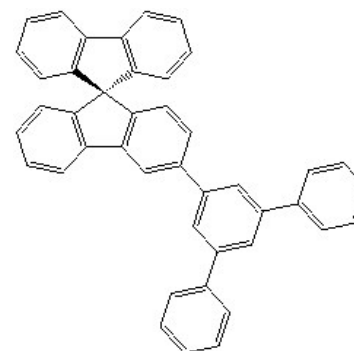
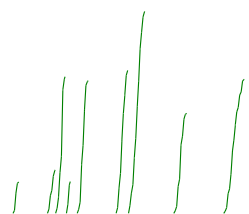
Table S16 The state-of-art device performance using universal hosts in red, green and blue PhOLEDs.

Compound	Red PhOLED		Green PhOLED		Blue PhOLED		EQE _{AV.}	Reference
	EQE _{max} [%]	CIE (x, y)	EQE _{max} [%]	CIE (x, y)	EQE _{max} [%]	CIE (x, y)		
4CzMC	11.4	(0.62, 0.38)	16.6	(0.32, 0.62)	18.9	(0.16, 0.31)	15.6	10
DPBP-DMAC	14.8	(0.68, 0.32)	23.8	(0.31, 0.63)	22.9	(0.19, 0.41)	20.5	11
DPMBP-DMAC	15.6	(0.67, 0.32)	24.7	(0.30, 0.64)	22.6	(0.19, 0.41)	20.9	11
<i>o</i> -CzTP	15.8	(0.60, 0.39)	25	(0.25, 0.64)	27.1	(0.15, 0.34)	22.6	12
BCPO	17	(0.67, 0.33)	21.6	(0.28, 0.65)	23.5	(0.13, 0.30)	20.7	13
2	17	(0.67, 0.33)	26.9	N/A	24.3	N/A	22.7	14
<i>m</i> -CzTP	17.2	(0.61, 0.38)	22.3	(0.26, 0.64)	23.9	(0.15, 0.33)	21.1	12
<i>o</i> -DiCzBz	20.1	N/A	20.4	N/A	27	N/A	22.5	15
TPA-L-BN	20.5	(0.61, 0.39)	20	(0.31, 0.64)	19.8	(0.16, 0.32)	20.1	16
1	20.5	(0.52, 0.48)	22.7	(0.35, 0.62)	16.1	(0.18, 0.32)	19.7	17
TCZSO ₂	21	(0.63, 0.37)	24	(0.35, 0.61)	22.8	(0.15, 0.35)	22.6	18
BII-TPA	22.1	(0.68, 0.31)	26.4	(0.34, 0.62)	21.2	(0.17, 0.34)	23.2	19
<i>m</i> -DCz-S	22.5	(0.50, 0.50)	22.6	(0.29, 0.64)	25.1	(0.15, 0.29)	23.4	20
BII-BCz	22.7	(0.68, 0.31)	27.8	(0.35, 0.61)	29.4	(0.16, 0.33)	26.6	19
4ICDPy	25.3	(0.67, 0.33)	27	(0.24, 0.64)	22.1	(0.14, 0.32)	24.8	21
<i>m</i>-STPh	27.3	(0.63, 0.37)	26.0	(0.32, 0.63)	27.1	(0.18, 0.38)	26.8	This work

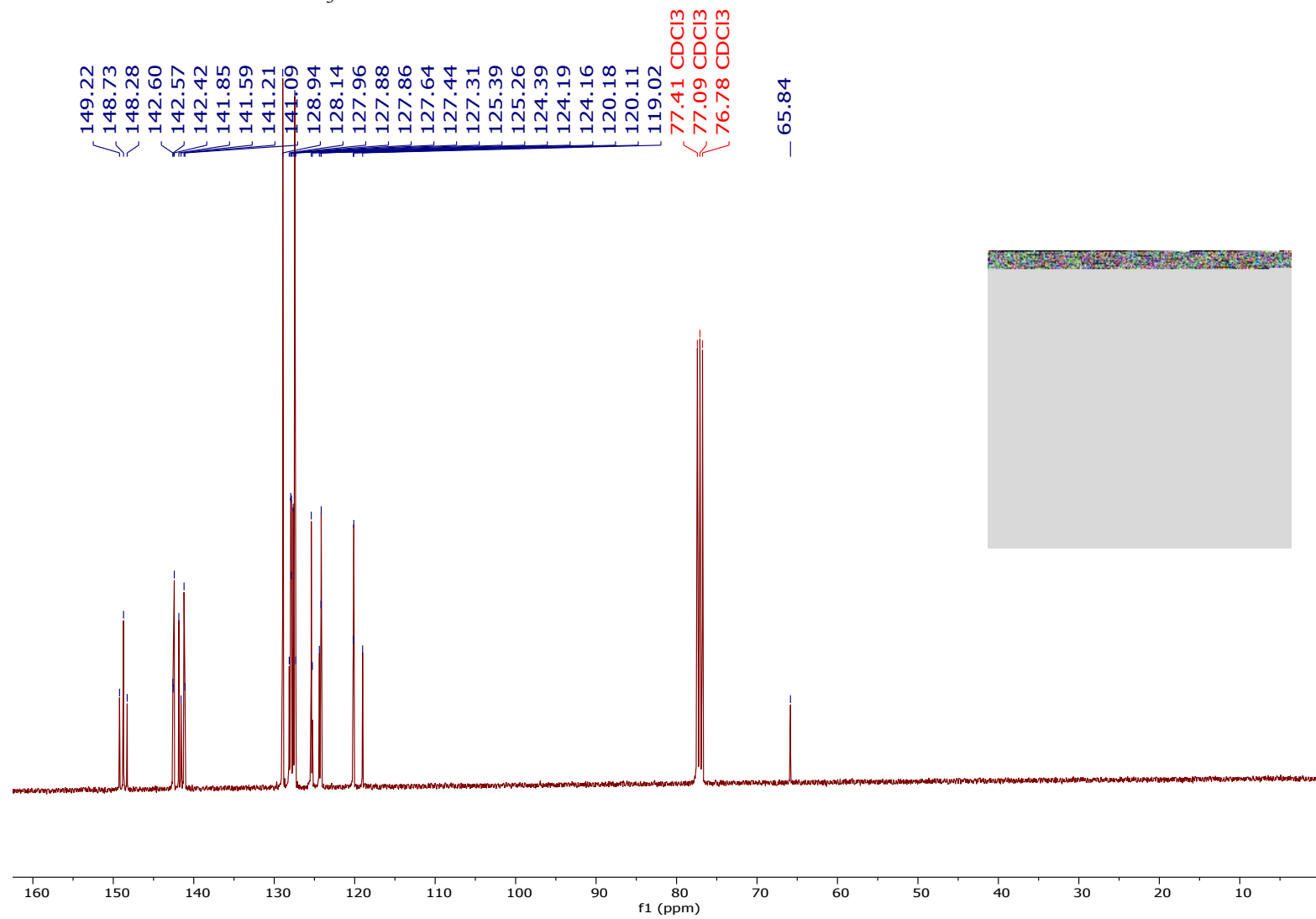
EQE_{AV.}: the average EQE value of each host in red, green and blue device performances.

10 Copy of NMR spectra

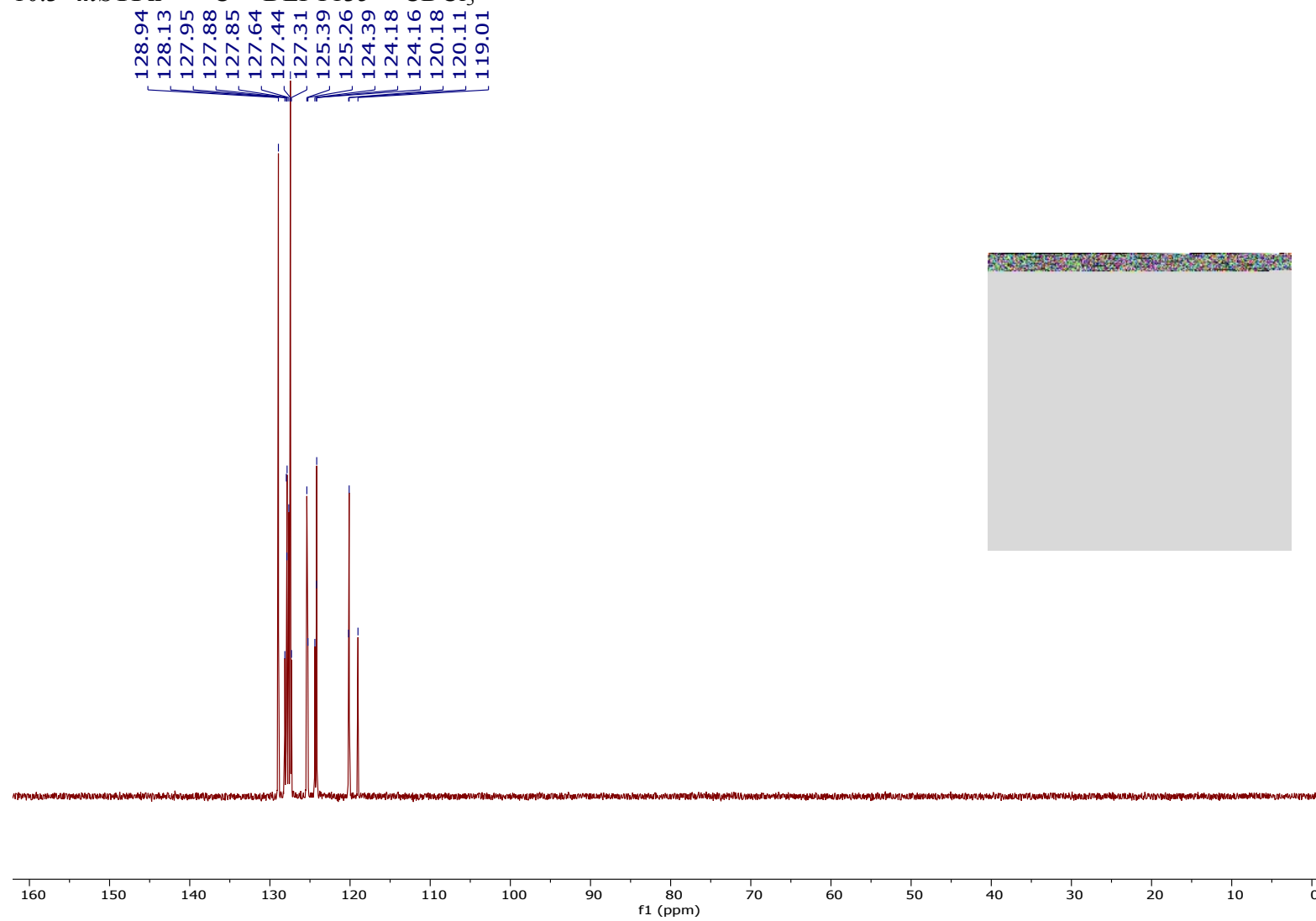
10.1 *m*STPh — ^1H — CDCl_3



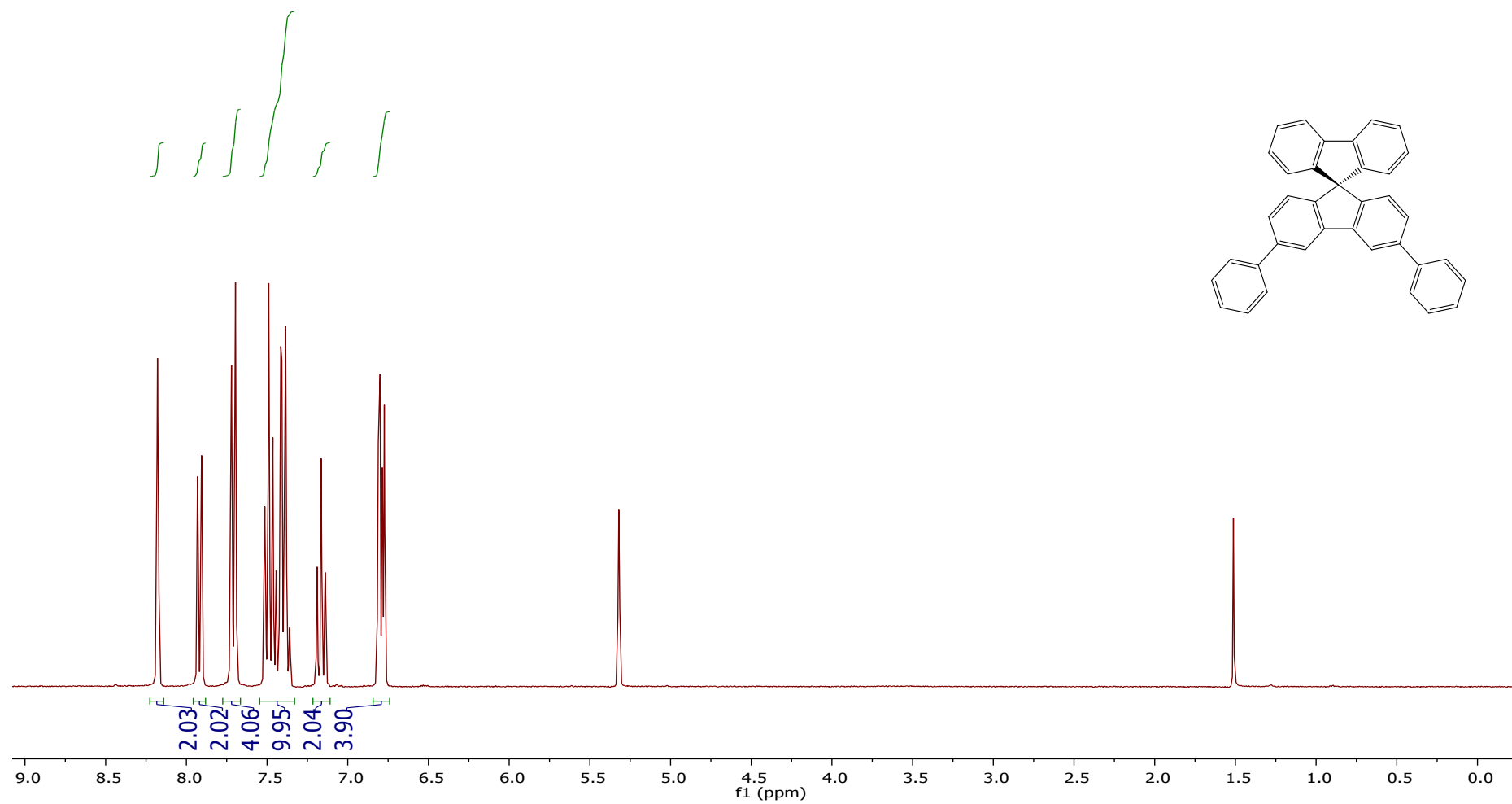
10.2 *m*STPh — ¹³C — CDCl₃



10.3 *m*STPh — ¹³C — DEPT135 — CDCl₃



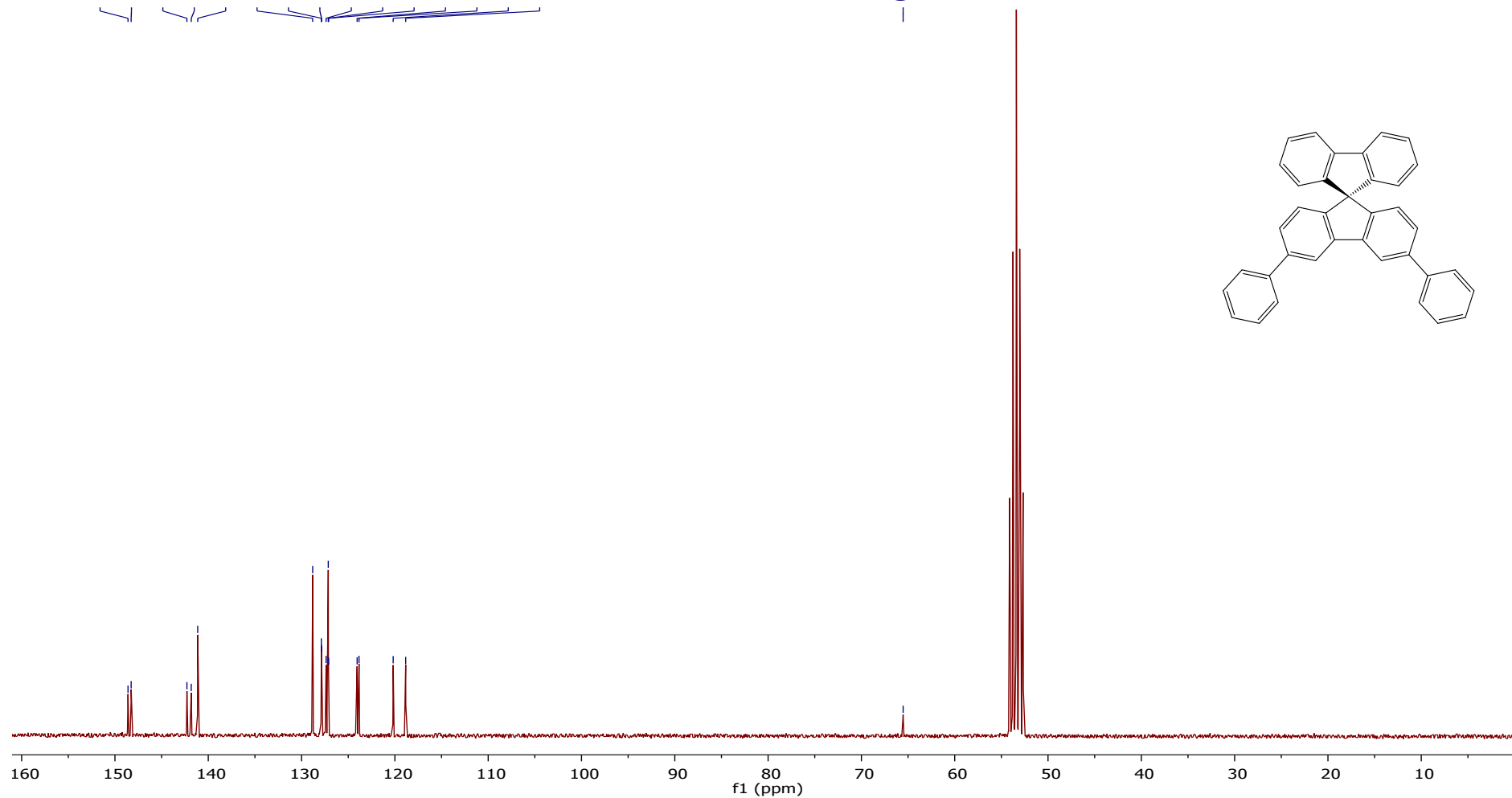
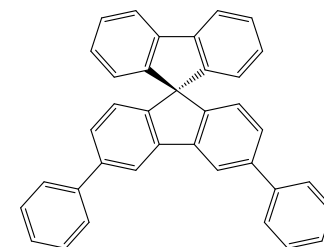
10.4 *m*SPh₂ - ¹H - CD₂Cl₂



10.5 *m*SPh₂ - ¹³C - CD₂Cl₂

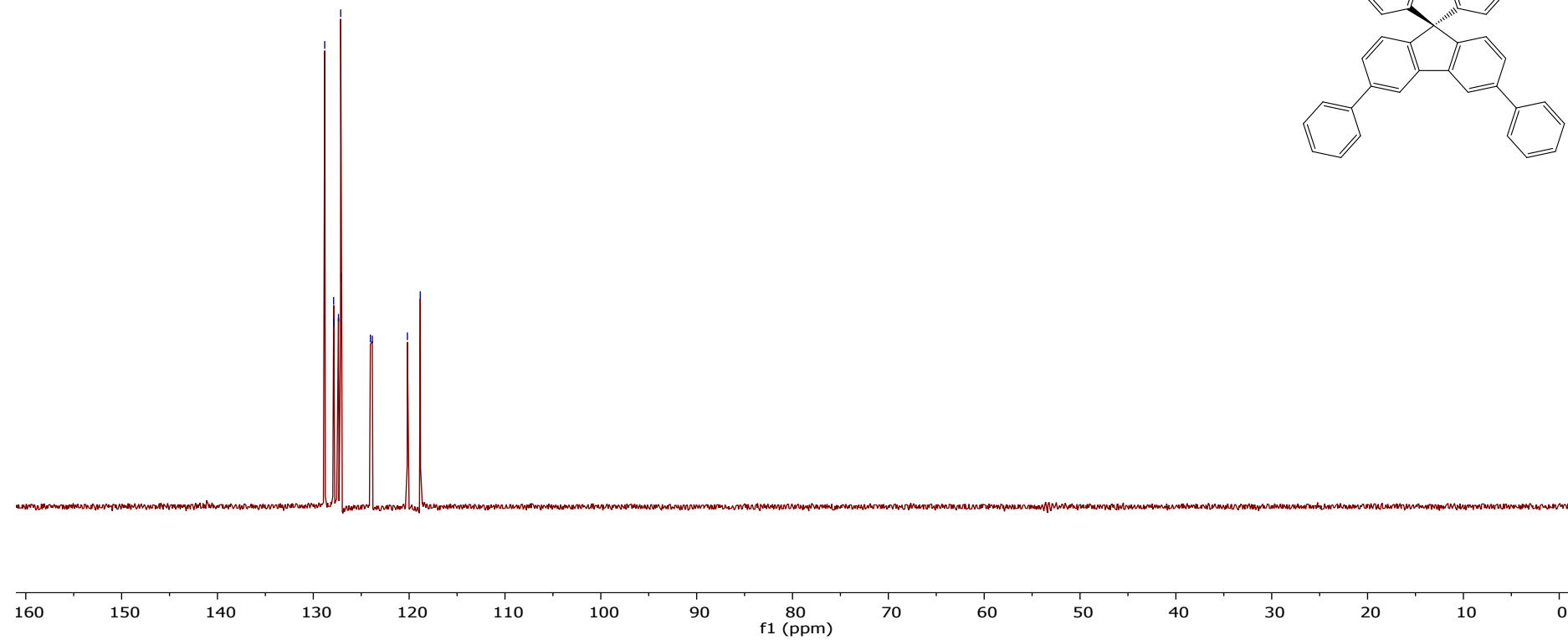
148.60
148.26
142.29
141.82
141.13
128.81
127.88
127.86
127.37
127.14
127.10
124.05
123.84
120.18
118.84

65.53

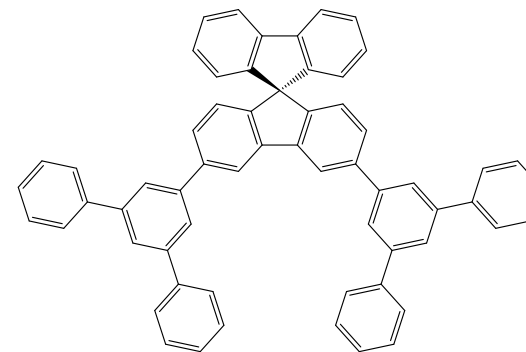
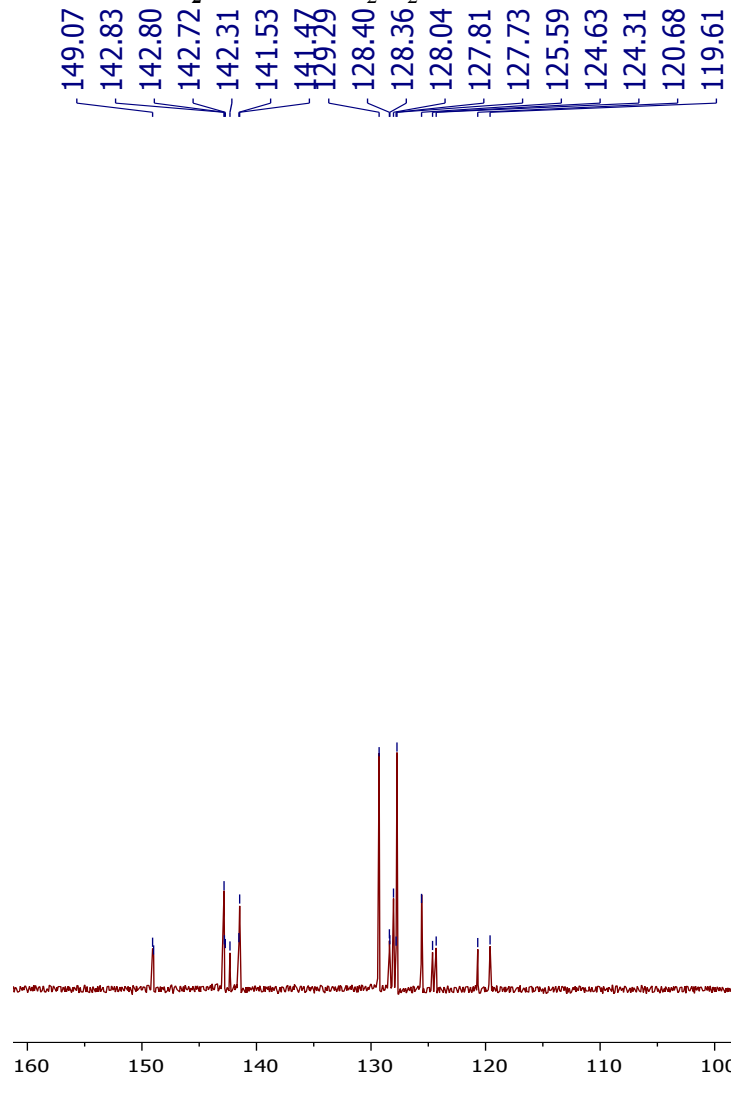


10.6 *m*SPh₂ - ¹³C - DEPT135 - CD₂Cl₂

128.81
127.88
127.86
127.37
127.14
127.10
124.05
123.85
120.18
118.84

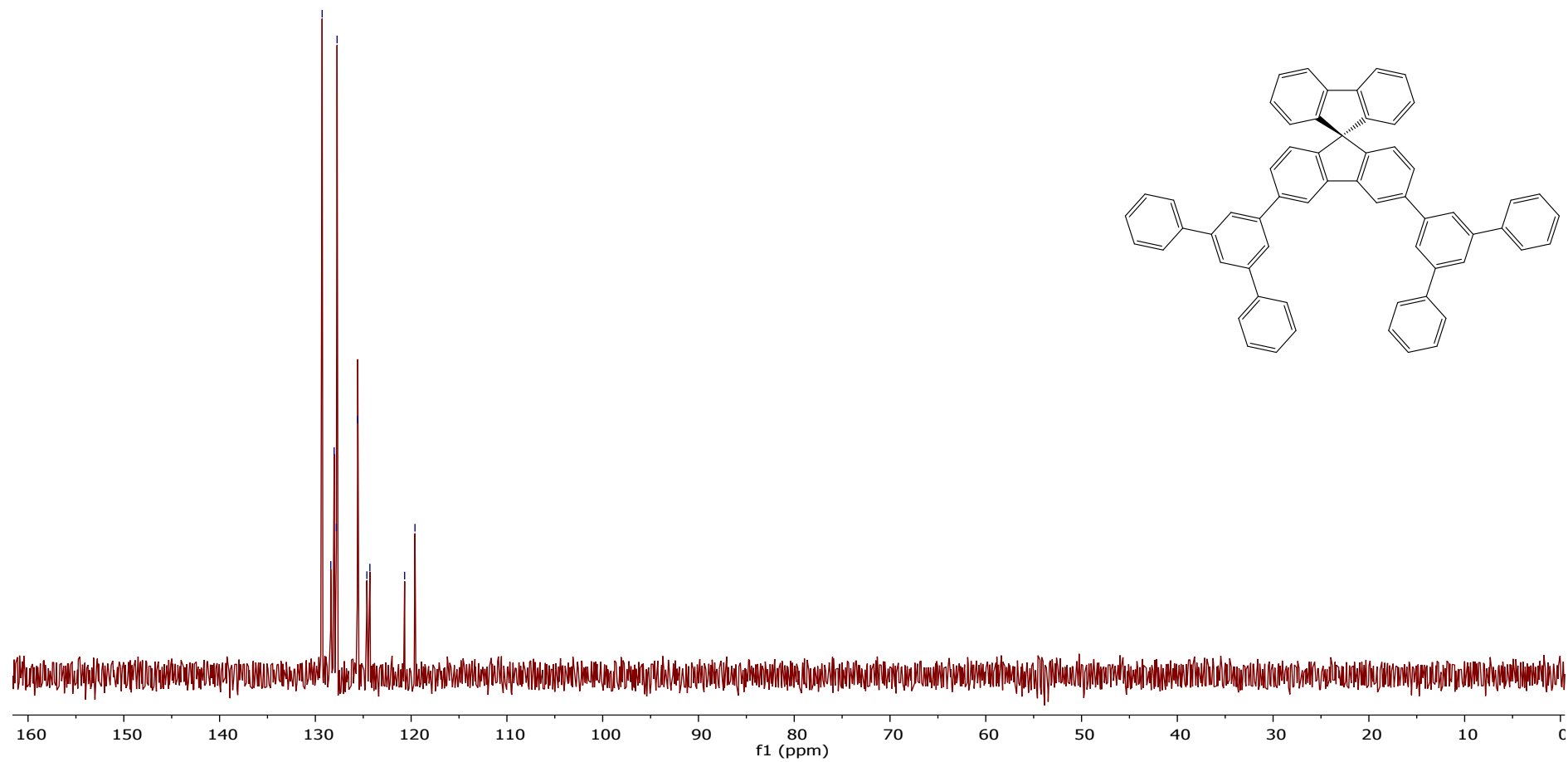


10.8 *m*STPh₂ - ¹³C - CD₂Cl₂



10.9 *m*STPh₂ – ¹³C – DEPT135 – CD₂Cl₂

129.29
128.39
128.04
127.80
127.73
125.58
124.62
124.31
120.68
119.60



11 References

1. G. R. Fulmer, A. J. Miller, N. H. Sherden, H. E. Gottlieb, A. Nudelman, B. M. Stoltz, J. E. Bercaw and K. I. Goldberg, *Organometallics*, 2010, **29**, 2176-2179.
2. C. M. Cardona, W. Li, A. E. Kaifer, D. Stockdale and G. C. Bazan, *Adv. Mater.*, 2011, **23**, 2367-2371.
3. A. P. Kulkarni, C. J. Tonzola, A. Babel and S. A. Jenekhe, *Chem. Mater.*, 2004, **16**, 4556-4573.
4. D. De Leeuw, M. Simenon, A. Brown and R. Einerhand, *Synth. Met.*, 1997, **87**, 53-59.
5. R. G. Parr, in *Horizons of Quantum Chemistry*, Springer, 1980, pp. 5-15.
6. P. Hohenberg and W. Kohn, *Physical review*, 1964, **136**, B864.
7. A. D. Becke, *Phys. Rev. A*, 1988, **38**, 3098.
8. A. D. Becke, *The Journal of chemical physics*, 1996, **104**, 1040-1046.
9. C. Lee, W. Yang and R. G. Parr, *Phys Rev B*, 1988, **37**, 785.
10. X. Qiu, S. Ying, J. Yao, J. Zhou, C. Wang, B. Wang, Y. Li, Y. Xu, Q. Jiang, R. Zhao, D. Hu, D. Ma and Y. Ma, *Dyes Pigm.*, 2020, **174**.
11. S. Hu, J. Zeng, X. Zhu, J. Guo, S. Chen, Z. Zhao and B. Z. Tang, *ACS Appl. Mater. Interfaces*, 2019, **11**, 27134-27144.
12. W. Song, L. Shi, L. Gao, P. Hu, H. Mu, Z. Xia, J. Huang and J. Su, *ACS Appl. Mater. Interfaces*, 2018, **10**, 5714-5722.
13. H.-H. Chou and C.-H. Cheng, *Adv. Mater.*, 2010, **22**, 2468-2471.
14. S.-J. Su, C. Cai and J. Kido, *Chem. Mater.*, 2011, **23**, 274-284.
15. J.-J. Huang, Y.-H. Hung, P.-L. Ting, Y.-N. Tsai, H.-J. Gao, T.-L. Chiu, J.-H. Lee, C.-L. Chen, P.-T. Chou and M.-k. Leung, *Org. Lett.*, 2016, **18**, 672-675.
16. C. Wu, B. Wang, Y. Wang, J. Hu, J. Jiang, D. Ma and Q. Wang, *J. Mater. Chem. C*, 2019, **7**, 558-566.
17. S. Gong, Y. Chen, J. Luo, C. Yang, C. Zhong, J. Qin and D. Ma, *Adv. Funct. Mater.*, 2011, **21**, 1168-1178.
18. X.-D. Zhu, Y.-L. Zhang, Y. Yuan, Q. Zheng, Y.-J. Yu, Y. Li, Z.-Q. Jiang and L.-S. Liao, *J. Mater. Chem. C*, 2019, **7**, 6714-6720.
19. W.-C. Chen, Y. Yuan, Z.-L. Zhu, Z.-Q. Jiang, S.-J. Su, L.-S. Liao and C.-S. Lee, *Chem. Sci.*, 2018, **9**, 4062-4070.
20. K. Gao, K. Liu, X.-L. Li, X. Cai, D. Chen, Z. Xu, Z. He, B. Li, Z. Qiao, D. Chen, Y. Cao and S.-J. Su, *J. Mater. Chem. C*, 2017, **5**, 10406-10416.
21. C.-C. Lai, M.-J. Huang, H.-H. Chou, C.-Y. Liao, P. Rajamalli and C.-H. Cheng, *Adv. Funct. Mater.*, 2015, **25**, 5548-5556.